Session 13

NOBLE GAS TREATMENT

WEDNESDAY: October 22, 1980
CHAIRMAN: Dwight W. Underhill
University of Pittsburgh

CONDITIONING AND STORAGE OF FISSION PRODUCT KRYPTON USING CONTINUOUS ION IMPLANTATION INTO SPUTTERED METALS

H.J. Schmidt[1,2], E. Henrich[1], F. Baumgärtner[3]
Kernforschungszentrum Karlsruhe

1) Institut für Heisse Chemie, 2) Institut für Angewandte Kernphysik
3) Technische Universität München, Institut für Radiochemie

Fed. Rep. Germany

Abstract

Krypton ion implantation into sputtered metals promises to offer improved safety during conditioning and storage or disposal of fission product krypton separated in spent fuel reprocessing plants, and has been investigated on a lab scale. Amorphous and crystalline metal deposits have been sputtered using an unsupported glow discharge at about 10^{-2} Torr in the annular gap between two concentric cylinder electrodes. The krypton was implanted into the continuously growing metal coating collected inside the outer cylinder. A sputtering voltage of about -3 kV was applied to the inner cylinder and an implantation voltage to the outer cylinder of either -0.3 kV for amorphous or about -1 kV for crystalline metal deposits. The end electrodes have been earthed. Amorphous Fe-Zr and Cu-Zr products contained up to 7 atom -% Kr. In crystalline Cu up to 5 and in crystalline Ti up to 8 atom-% Kr have been determined. The minimum power consumption for the implantation process corresponded to about 10 ppm of the reprocessed reactor power for the amorphous alloys and to about 20 ppm for crystalline Ti. Material and power consumption are reasonably low.

In the amorphous alloys a monoatomic krypton distribution is suggested from neutron scattering results. In the crystalline Cu or Ti the Kr is contained in small bubbles.

The thermal release rates of the Kr containing coatings have been determined in a linear temperature gradient up to 10^3 °C and at constant temperatures until steady state conditions were obtained at higher temperatures. The small initial low temperature release rates were found to decrease with time, additional coating with the pure metal or thermal annealing at higher temperatures. They have been therefore associated with the release from the surface regions. The extrapolated thermal release rates for amorphous Fe-Zr and crystalline Ti samples have been determined, being 1% in 100 years at temperatures $\leq 400^{\circ}C$ and $\leq 0.1\%$ in 100 years at $\leq 300^{\circ}C$.

I. Introduction

In future it will be necessary to remove most of the fission product krypton from the dissolver off-gas in spent fuel reprocessing plants. The storage of the separated krypton in high pressure cylinders includes the risk of rapid accidental release of relatively large inventories. Encapsulation in zeolites (1) gives a superior waste form, which can be stored at atmospheric pressure. The discontinuous

encapsulation process requires the accumulation of radioactivity in unconditioned form as well as high pressures and high temperatures. The final waste form has considerable thermal, chemical, and radiation mechanical stability. But the large surface is not favourable in view of chemical attack or thermal release.

The fission product krypton implantation into sputtered metals proposed by Harwell [2], UK, in 1974, does not have these disadvantages. The implantation process operates continuously at subatmospheric pressure and about normal temperature; an accumulation of large inventories is not necessary. The final waste form is a compact piece of metal without a large surface having a storage capacity of about 200 ± 100 l Kr per l of metal. By suitable choice of material considerable thermal, chemical, mechanical and radiation stability will be obtained to satisfy the safety requirements for transport, storage or disposal. The main problems are expected to come from the use of a high voltage and a high power density, necessitating controlled cooling to maintain low temperatures.

A suitable arrangement for a technical application is a glow discharge as a Kr ion source in the annular gap between two concentric metal cylinders being isolated from each other. At a cylinder distance of a few cm and a Kr pressure less than about 0.1 Torr the system can act as a self-sustaining Kr pump.

Different operating modes have been used and are comparable to the operation of a triode ion sputter pump [3,4,5,6]. During the discharge material is gradually sputtered from the inner cylinder and deposited inside the outer cylinder. Kr ions from the glow discharge are trapped in the growing metal deposit. Before the inner electrode cylinder is used up, the implantation unit has to be replaced by a new one. The electrical power density at the electrode surfaces amounts to several Watt/cm^2, and has to be removed by cooling.

A 50 kW pilot plant has been built in Harwell/ UK [5], using a self-sustaining Kr glow discharge. The discharge polarity was reversed in about sec-periods by a specially developed high power-high voltage thyratron switch. Most of the period the large negative potential was applied to sputter the inner cylinder, within a shorter time the Kr ions were implanted into the freshly sputtered metal by reversing polarity. Repeating the switching process, a thick metal deposit was built up. Well known commercially available and less expensive metals (eg. Cu) or alloys forming suitable crystalline deposits will be prefered.

A more convenient continuous mode of operation, without the periodical reverse of polarity has been used at PNL/USA. To implant the Kr in glassy metal alloys a potential of -2 ÷ 3 kV was applied to sputter a mixed inner cylinder and an implantation potential of only -0.2 ÷ 0.3 kV to the glassy metal alloy deposit formed inside the outer cylinder; the isolated end caps have been earhed to remove the electrons. The glow discharge was supported by electrons from a hot filament (thermionically supported plasma), thus reducing discharge pressure and energy loss due to backsputtering. Using glassy metal alloys and a continuous electron supported glow discharge high Kr concentrations up to 10 atom% and a considerably reduced power

consumption were obtained.

In this work we have tried to combine the more convenient continuous mode of operation to well known commercially available crystalline metals. Moreover, the discharge was not supported by electrons from a hot filament. The main reasons are: 1. filament burn out in a hot plant area due to air break through concerning an otherwise impurity insensitive process and 2. additional complication of electrode fabrication.

II. Experimental

1. Implantation procedure

The triode sputtering system shown in fig. 1 was used. The metals or alloys were sputtered from the inner (4 cm diameter) of two water cooled concentric cylinders to the inside surface of the outer cylinder (10 cm diameter) by a self sustaining unsupported krypton glow discharge.

A negative voltage up to 4 kV was applied to sputter the inner cylinder, a negative implantation voltage up to 1 kV to the outer cylinder. By this way the Kr was implanted continuously into the growing metal coating. The electrons were removed by the grounded endelectrodes.

In order to get Kr containing crystalline metals a homogeneous sputter electrode was used. In the case of amorphous coatings holes were drilled into the sputter electrode. Cylindric slugs of the minor component metal were then pressed into the holes. As an alternative method milling of perpendicular grooves into the sputter electrode and pressing strips of the minor component metal into the grooves was used. By these methods Fe-Zr and Cu-Zr sputter electrodes were made (fig. 2).

2. Characterization of krypton implanted deposits

X-ray and neutron diffraction measurements demonstrated the crystalline or amorphous structure. In the case of amorphous Fe-Zr-Kr samples inelastic neutron scattering experiments were made to investigate in which form the krypton is distributed in the amorphous samples.

By scanning electron microscopy (SEM) the structure of the samples before and after thermal annealing was studied.

The thermal release was followed by heating the coatings up to 10^3 °C in a linear temperature gradient of 10 °/min. The steady state release rates were determined by heating the samples at constant temperature in steps of 100°C up to 500°C until steady state release conditions could be observed (fig. 3). Depending on the amount of deposit the upper detection limit was 10^{-2} to 10^{-1} % Kr-release/year.

III. Results and discussion of the implant process

1. Coating growth rates

Depending on sputter- and implantation parameters coating growth rates up to $1.5 \cdot 10^{-6}$ g/cm^{2}sec for amorphous Fe-75/Zr-25, Fe-40/Zr-60, Cu-60/Zr-40 and crystalline Ti samples were detected. This corresponds to about two grams/hour.

2. Krypton concentrations

Kr-concentrations up to 8 atom% (table I) were found by melting the samples in the gas release detection system or by the weight loss and detecting the increase in Kr-partial pressure as well as by the pressure drop of the implantation gas inlet system. Depending on the sample this corresponds to amounts up to about 200 Nml-Kr/cm^3.

3. Power consumption

In the case of the amorphous deposits we observed a minimal power consumption at implantation voltages of 0.3-0.4 kV (fig. 4). The pumping rate increased about linearly with discharge pressure (fig. 5) equivalent to the ion current. The minimal power consumption of 30 kWh/Nl-krypton has been obtained at pumping rates of 20-30 Nml/h. Depending on sputter- and implantation voltages we measured pumping rates up to 40 Nml/h at twice the high power consumption.

At implantation voltages of 0.9-1 kV we obtained similar results for the crystalline Ti,Cu -Kr samples. The minimal power consumption was about 60 kWh/Nl -krypton. This is equivalent to 20 ppm of the reprocessed reactor power. Within certain limits the implantation rate can therefore be adjusted to the output of the separation plant without accumulating radioactive Kr.

4. Influence of oxygen or nitrogen contaminants

Adding up to 60 vol% O_2 or N_2 to Kr a slight decrease in the minimal power consumption for amorphous samples (fig. 6) was observed. Within our experimental accuracy no influence to thermal Kr release rates has been found. We found that oxygen and nitrogen are so easily embedded in the amorphous deposit, that the pumping rate of the gas mixture up to about 15 vol% O_2 and N_2 in Kr increased and then slowly decreased. The pumping rate refered to Kr changed corresponding to fig. 6. This effect is expected to be attributed to the stabilisation of the amorphous structure by the small oxygen or nitrogen atoms.

In the case of crystalline Ti-Kr-coatings preliminary experiments with 20 vol% air in Kr showed no influence on power consumption, pumping rate and thermal Kr-release rates.

No sophisticated precleaning steps therefore seem to be necessary in a fission product krypton implantation plant for amorphous as well as for crystalline deposits.

IV. Characterization of products

1. Amorphous deposits

Chemical analysis. The analysis showed that the Fe/Zr-and Cu/Zr-ratio was within 10% identical with the composition of the sputter electrode area.

Inelastic neutron scattering. The phonon density of states was determind using neutron inelastic scattering. For a $(Fe\text{-}40/Zr\text{-}60)_{93}Kr_7$ sample an increase of intensity in the neutron spectra between 2 and 20 meV could be detected which peaks at about 10 meV[5]. If the Kr is contained in form of small bubbles it has to be in the liquid state since the pressure necessary to hold such amounts of Kr is far above its critical pressure. For solid Kr the frequency spectrum peaks around 4 meV and ends at 6 meV [7]. This means that the dynamical forces we measured are about a factor of 10 larger than for solid Kr. However, for the liquid state the dynamical forces should be rather weak as they are for the Van der Waals type [8]. These results suggest that the Kr-atoms are distributed on single sites in the amorphous lattice.

Density. For a monoatomic distribution inside the holes between the metal atoms one might expect a somewhat higher density for samples with a higher Kr-content. For Fe-40/Zr-60 with 7 atoms% Kr we have measured a density of $\delta = 6.5 \pm 0.05$ g/cm^3 and $\delta = 6.86 \pm 0.05$ g/cm^3 for a sample with 1 atom% Kr. Assuming that the model of dense random packing of hard spheres applies in our case the lower density of the Kr-rich sample means that larger holes are between the atoms than in the 1% case. This suggests that the Kr-atoms are a part of the amorphous matrix and not host-atoms in the holes between metal atoms.

Thermal Kr-release rates. It is very reasonable to assume that significant Kr-release occures if the matrix is destroyed by crystallization. This should not happen if the heat caused by the radioactive decay can be removed by heat conduction in the amorphous metal. The radioactive decay, however, should not influence the amorphous state [9].

Thermal release measurements showed a very low release up to 400°C (fig. 7). The release rates decreased as a function of time. After a period of 50-100 h steady state was reached. The total Kr-amount released up to steady state was less than 0.1%. The release at $T > 400$°C is correlated with crystallization. No changes of the glassy structure after a period of 100 h at 400°C could be detected using raster electron microscop scanning. The extrapolated release in 10 years will be $\leq 0.1\%$ at temperatures ≤ 400°C.

Differential thermo analysis (DTA). Preliminary results in DTA measurements showed no detectable heat emission up to 1000°C if the measurements were undertaken in argon atmosphere to avoid oxidation effects.

2. Crystalline Cu-Kr and Ti-Kr deposits

Density. Under the assumption that in crystalline metals the Kr is

contained in small bubbles rather than in a monoatomic distribution, the Kr has to be in the liquid state. With the partial densities of $\delta_{Kr} = 2.6$ g/cm^3 and $\delta_{Ti} = 4.5$ g/cm^3 one arrives at a density of $\delta = 4.35$ g/cm^3 for the $Ti_{92}Kr_8$-system. This compares very well with the value we have determined for our deposit being 1/2% less.

Krypton release. From the extrapolated steady state Kr-release rates shown in fig. 8 and 9 one can see that the total amount of Kr would have left the Cu-matrix if it had been kept at 400°C for 1 year. In contrast only 1% of the Kr would have been released from the Ti-matrix at the same temperature in 10 years.

The high release of Kr from Cu can be attributed to the onset of self diffusion of Cu-atoms at about 400°C, whereas self diffusion of Ti-atoms due to the melting point of 1668°C starts at higher temperatures.

To get reliable low temperature release data we have also measured the release behaviour of $Ti_{92}Kr_8$ -samples over a period of 10^3 h. In all cases the release up to 400 °C was less than 0.1% of the total amount. A sample which was held at various temperatures up to 550°C for the same time showed a release of 0.7%.

Sudden Kr-pressure increases were observed at temperatures above 300°C for Cu- and above 500°C for Ti-matrices. Raster electron microscope pictures of the same samples showed bursted bubbles at the surface of the materials after this heat treatment (fig. 10).

Further measurements on Ti-samples showed that the release rate decreased below the detection limit after approximately ten hours if the temperature had not increased above 500°C. However, if the temperature was raised above 500°C for some minutes only and then reduced to lower temperatures again, steady state release rates as high as 5-10 %/y have been measured. This can probably be attributed to the interconnection of bubbles in form of channelsystems which form irreversibly above 500°C. The sizes of these interconnections seem to be dependent on temperature. In fact interconnections with various sizes were detected in bursted bubbles after a heat treatment up to 1000°C using a raster electron microscope (fig. 10b).

Fracture of deposits. In order to investigate how many krypton will be released if a mechanical fracture of the matrix occurs a Cu-deposit was fractured in our gas release detection system. The deposit had been annealed at 300°C and contained 3 atom-% Kr. The amount of Kr released corresponded to a depth of 100 Å from the fresh surface. In the same measurements with amorphous $(Fe\text{-}40/Zr\text{-}60)_{93}Kr_7$ the release was less than the detection limit of about 20 Å, supporting the neutron scattering results.

V. Extrapolated plant application

Reprocessing plant capacity may be achieved by parallel operation of several implantation units. Normal operating conditions should guarantee minimum power consumption. Accumulation does not occur if the installed krypton implantation capacity corresponds to the maximum dissolution rate. Breakdown of a unit can be compensated on-line; the pumping rates of the other units are increased, operating slightly beyond optimum conditions.

At the end of their useful life the proposed 50 - 100 kW pilot units contain about the same inventory as pressurized cylinders. The implantation process can be designed to operate remotely under automatic control; manpower is required during the replacement of spent units to connect and disconnect electric power, cooling water and vacuum pumps. Additional preparation for transport, storage or disposal might be necessary. The number of handling procedures is proportional to the number of spent units and not to the number of units in parallel operation.

VI. Conclusions

Compared to other alternatives, ion implantation into sputtered metals promises to offer improved safety for conditioning and storage of fission product krypton. The continuous process operates at subatmospheric pressure and ambient temperature and can be made to operate automatically and without Kr accumulation. The freedom of choice of a metal matrix guarantees the adaptation to the storage environment. The final waste form can be stored at atmospheric pressure. Depending on the metal matrix, considerable thermal, mechanical radiolytic and chemical stability can be obtained.

The energy consumption corresponds to about 10 - 20 ppm of the reprocessed reactor power; less than 2 l of storage metal is required per ton of spent fuel. The manufactoring requirements for the implantation units are conventional.

Neither the implantation process nor the product quality require a high purity of krypton, thus simplifying the separation process. Comparing the alternatives ion implantation is possibly a somewhat more but still reasonable expensive method offering improved safety, compatibel with ALARA criteria and public acceptance.

Acknowledgements

We gratefully acknowledge the support of this work by Prof. Dr. W. Schmatz, Institut für Angewandte Kernphysik, Kernforschungszentrum Karlsruhe and Dr. J.B. Suck for the critical reading of the manuscript.

References

(1) R.D. Penzhorn; Alternativverfahren zur Kr-85-Endlagerung KfK 2482, 1977

(2) R.S. Nelson, S.F. Pugh, M.J.S. Smith, D.W. Clelland; British patent No 1, 485, 266, filed 1974

(3) G.L. Tingey, E.D. MacClanahan, M.A. Bayne, W. Gray; JAEA-SM- 245/31, 1980

(4) E. Henrich, H.-J. Schmidt; Proc. of Reaktortagung Berlin 1980

(5) D.S. Whitmell, R.S. Nelson, M.J.S. Smith; JAEA-SM- 245/7, 1980

(6) H.-J. Schmidt, E. Henrich, T. Fritsch, F. Gompf, B. Renker and E. Mohs
Proceedings of the IV Intern. Conf. on Liquid and Amorphous Metals, Grenoble 1980

(7) F. Gompf, B. Renker, H.-J. Schmidt in Progress Report 1979/80 ed. by V. Jung and V. Österreich, JAK-KfK

(8) J. Skalyo, Y. Erdoh, G. Shirame;
Phys. Rev. B9, 1797 (1974)

(9) H.-J. Güntherodt;
Metall 7,33 p. 732 (1979)

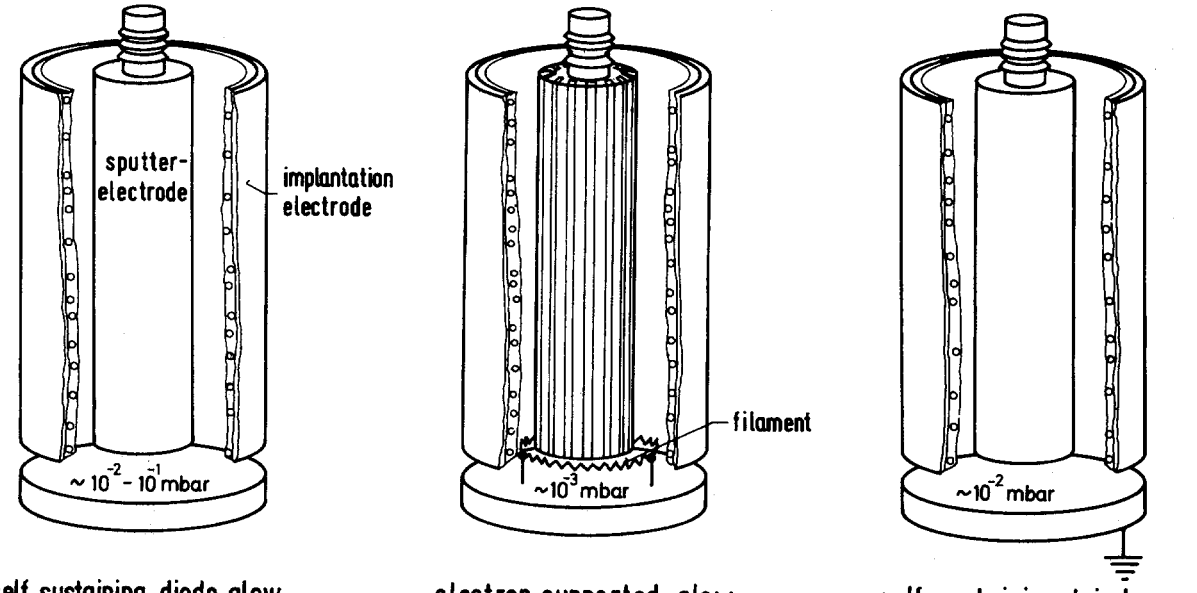

Fission product krypton implantation procedures

Fig. 1

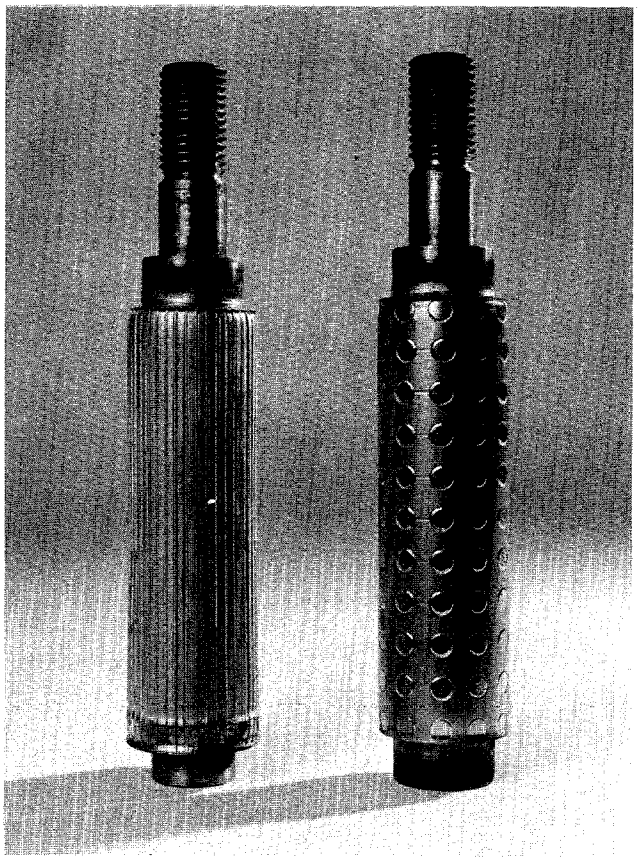

Fig. 2

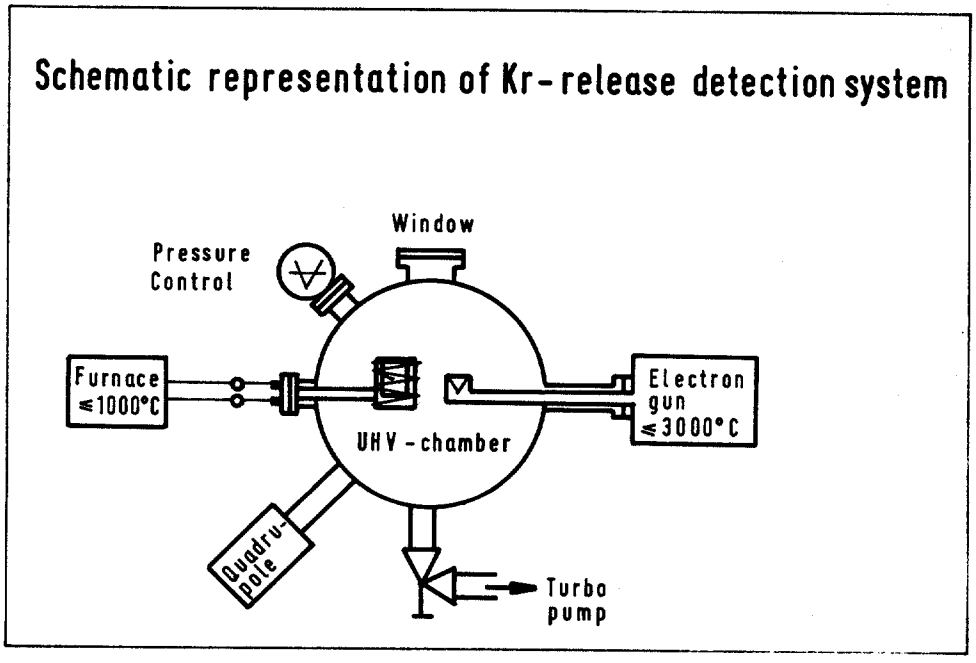
Schematic representation of Kr-release detection system
Window
Pressure Control
Furnace ≤1000°C
Electron gun ≤3000°C
UHV-chamber
Quadru-pole
Turbo pump

Fig. 3

Pumping rate vs. discharge pressure.

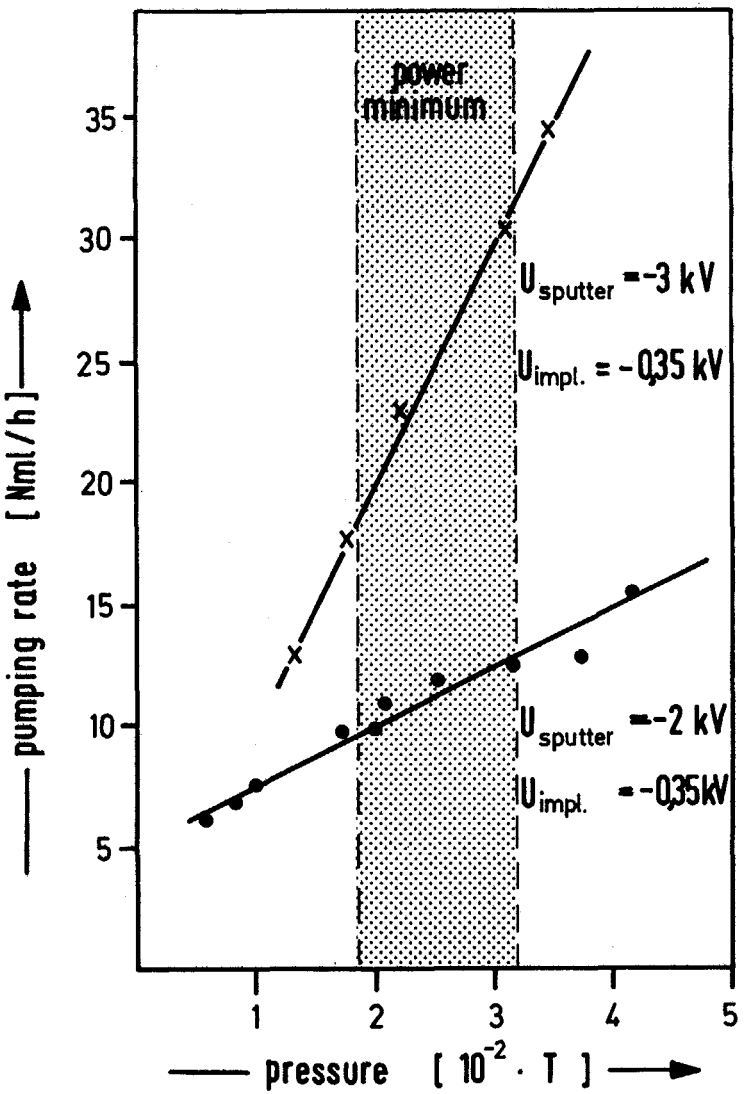

Fig. 5

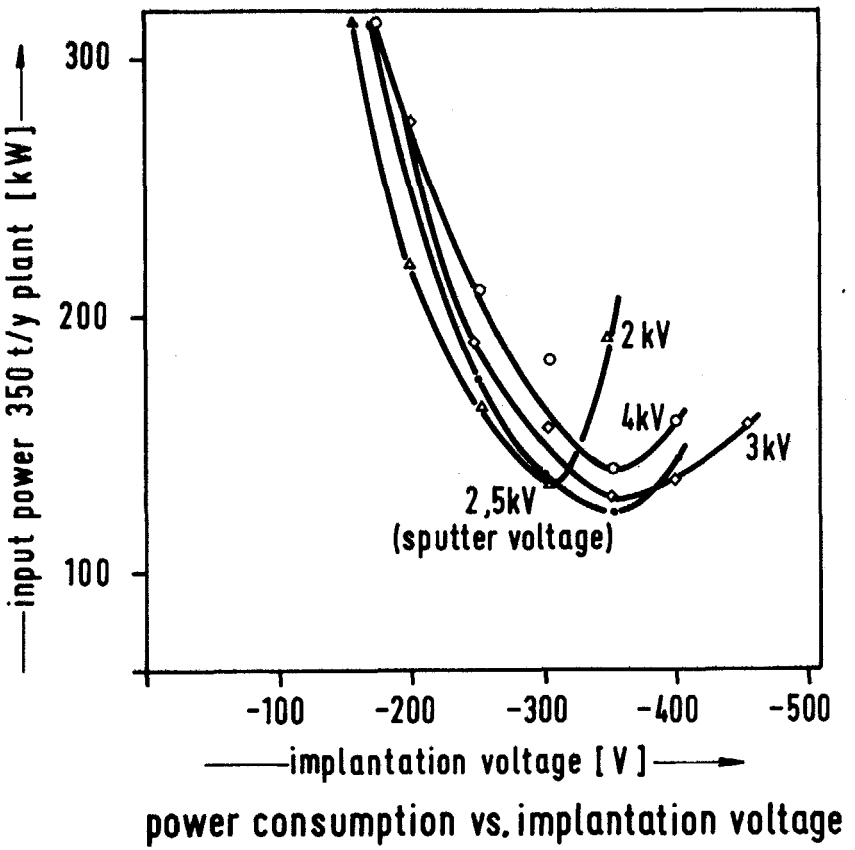

power consumption vs. implantation voltage

Fig. 4

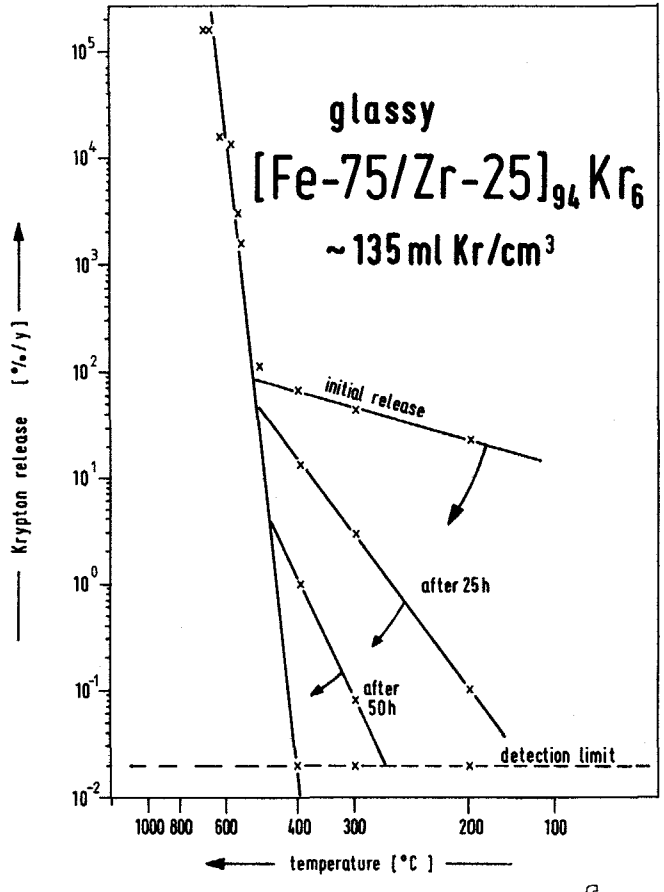

Steady state krypton release rates

Fig. 7

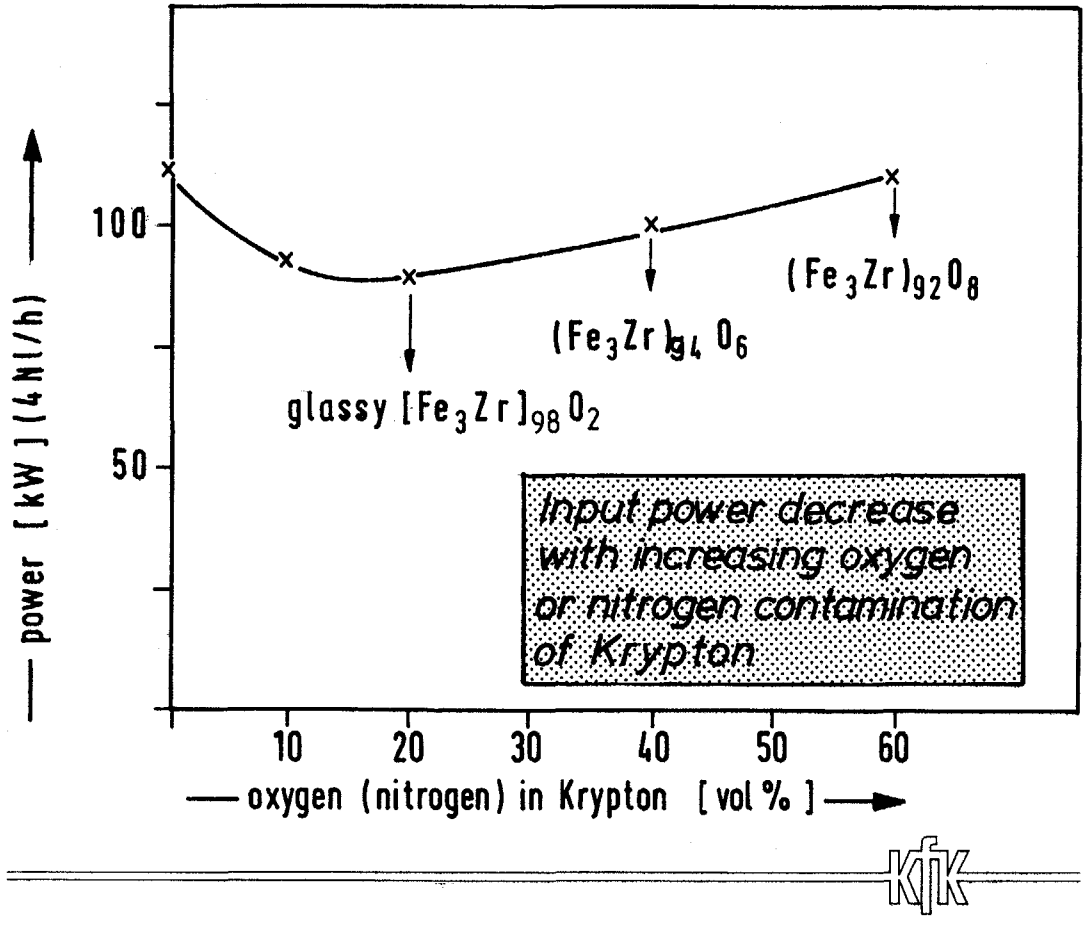

Change in electrical input power with oxygen or nitrogen contamination of Kr

Fig. 6

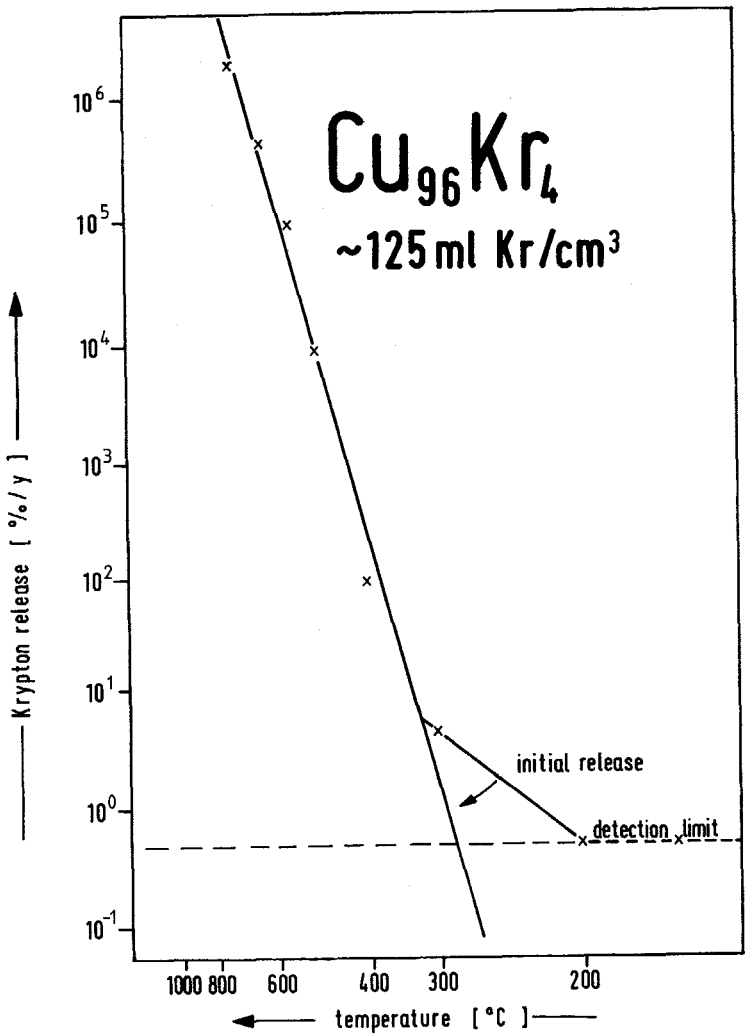

Steady state krypton release rates

Fig. 8

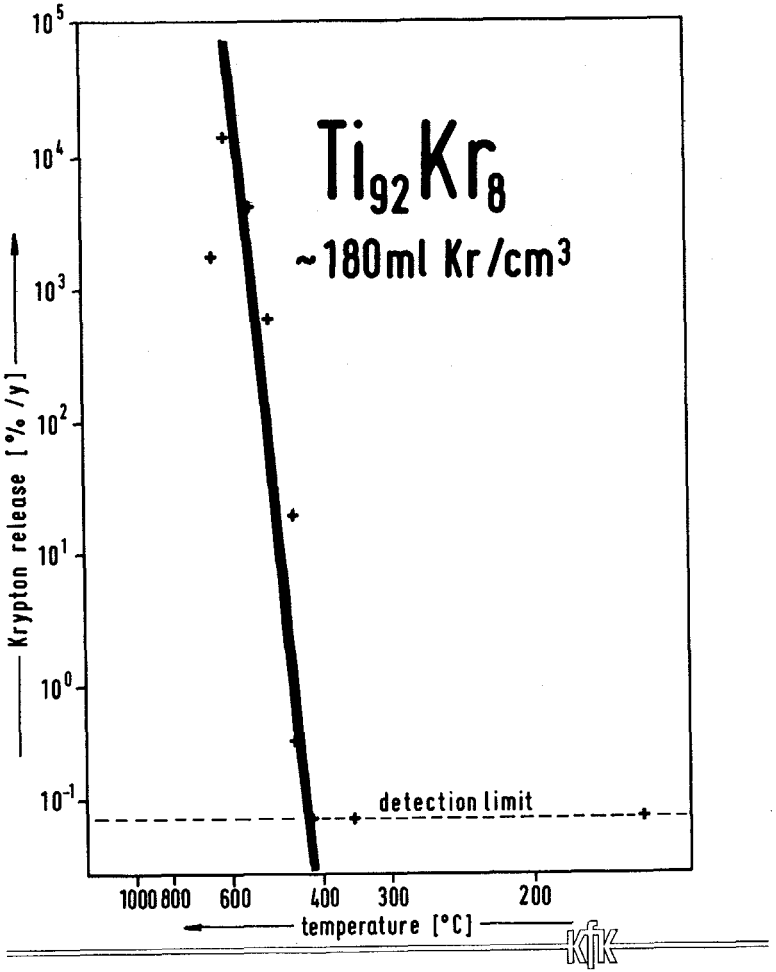

Steady state krypton release rates

Fig. 9

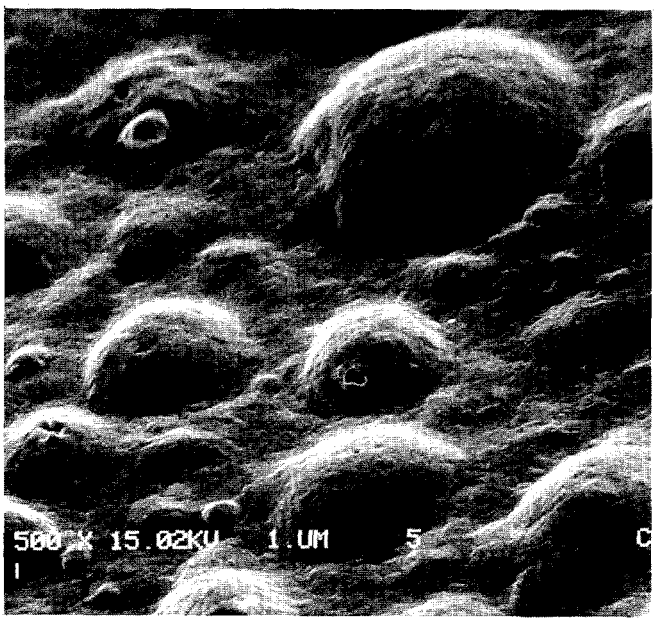

Fig. 10a

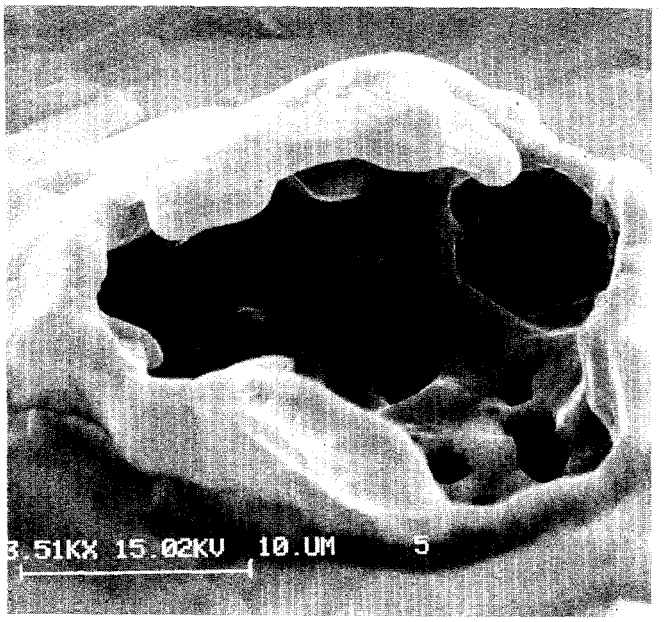

Fig. 10b

	HARWELL[5]	PNL[3]	this work
DISCHARGE TYPE MODE	SELF SUSTAINING DIODE (TRIODE)	ELECTRON SUPPORTED TRIODE	SELF SUSTAINING TRIODE
PROCESS	PULSED	CONTINUOUS (PULSED)	CONTINUOUS
PRODUCTS	<u>crystalline</u> $Fe_{95}Kr_5$, $Cu_{95}Kr_5$ etc.	<u>amorphous</u> $Fe_{79}Y_{12}Kr_9$, $Ni_{76}Y_{12}Kr_7$, $Zr_{68}Fe_{24}Kr_8$ etc. <u>crystalline</u> (pulsed) $Ni_{95}Kr_5$, $Fe_{95}Kr_5$, $Al_{96}Kr_4$, $Ti_{96}Kr_4$ etc.	<u>amorphous</u> $(Fe_2Zr_3)_{93}Kr_7$, $(Cu_7Zr_3)_{93}Kr_7$, $(Fe_3Zr)_{93}Kr_7$ etc. <u>crystalline</u> $Cu_{97}Kr_3$, $Ti_{92}Kr_8$ etc.
ENERGY CONSUMPTION (kWh/Nl)	$Cu_{95}Kr_5$ ~70	amorphous deposits ~20-30 $Ni_{95}Kr_5$ ~55, $Fe_{95}Kr_5$ ~50 $Al_{96}Kr_4$ ~130, $Ti_{96}Kr_4$ ~140	amorphous deposits ~30 $Cu_{97}Kr_3$ ~70, $Ti_{92}Kr_8$ ~60

<u>Tab. 1</u>

DISCUSSION

MARSHALL: This is perhaps more a comment than a question. Dr. Whitmell from Harwell, who has been in the U.S. recently, could not come today to give a paper on his method, which you described at the beginning of your talk. But he thought that some of you might like to know the current state of his system. He has been running his pilot plant now for about 1200 hours at 30 KW with an implantation rate of about 0.3L/hr. and he has got a deposit now about 15mm thick and it is still building up to his design specification of about 20mm. I wondered, along that same line, what sort of deposit thickness you have achieved so far. How thick a layer have you produced in your system?

HENRICH: Up to now we have been operating without automatic control. In our about 100 hour runs, the sample thickness was $\leq$ 1 mm.

LONG-TERM STORAGE OF Kr-85 in ZEOLITE 5A[+]

R.-D. Penzhorn
Institut für Radiochemie
Kernforschungszentrum Karlsruhe, Postfach 3640
7500 Karlsruhe, Federal Republic of Germany.

1. Abstract

From experiments on the fixation of Ar, Kr and Xe in the temperature range 400-550°C and pressures between 100 and 2000 bar in zeolites of type A, it was discovered that, when the zeolite is exchanged with divalent cations (Mg, Ca and Sr), the encapsulated noble gas brings about a collapse of the crystalline structure (glassification or sintering?). This effect is essentially independent of the amount of gas sorbed. In addition, the zeolite containing trapped gas looses its ability to sorb H_2O, CO_2 and other gases. Since a reloading after desorption at elevated temperatures is not possible, it may be concluded that the alteration of crystal structure after encapsulation is permanent. The obtained product has remarkable properties with regard to the long-term storage of Kr-85, i.e. no significant gas leakage is apparent even after 8 month at 450°C, several days of storage under water or irradiation with γ-rays within the dosis range $0.3\text{-}3.0 \times 10^8$ rad.

Systematic experiments were carried out to optimize the encapsulation. In this context the effect of the cationic composition, the pretreatment, the fixation temperature, the fixation pressure, the type of noble gas, etc. was examined. The results indicate that an adequate loading (20-30 cm^3 STP Kr/g) can be obtained at 520°C and pressures well below 500 bar. A further improvement can be achieved with a monolithic block (density increase by a factor of about 2).

It was demonstrated that, instead of mechanical compression, cryogenic pumping followed by PVT compression can be employed for the encapsulation of Kr. The result is a simplified process with improved safety.

[+]Supported in part by the Commission of the European Communities under its program on radioactive waste and storage.

2. Introduction

Since regulations in the Federal Republic of Germany have limited the amount of Kr-85 that can be released to the atmosphere during reprocessing of spent nuclearfuel, there is considerable interest in the development of technology for the long-term storage of this radioactive noble gas. The most obvious form of storage would be in standard pressurized gas cylinders placed in an appropiate storage facility. However, the high costs as well as the potential dangers caused by an eventual corrosion or accidental cylinder damage have stimulated research devoted to investigate wether Kr-85 can be immobilized in a solid matrix.One alternative, which consists in the trapping of radioactive Kr in the internal crystal framework of a zeolite has been under investigation in ENI, Idaho for several years 1/ and more recently in KfK, Karlsruhe 2/.The work carried out in Karlsruhe appears to indicate that zeolites of type 5A have considerably better characteristics for the long-term trapping of Kr than any other zeolite currently under investigation. This conclusion is primarily based on the better sorption kinetics and high stability towards elevated temperatures of this trapped noble gas/zeolite system. The result of the comparatively low leakage is a higher tolerable loading during final storage, coupled to a reduction in waste volume. The consequence of the faster sorption kinetics and the higher loading capacity is, that the encapsulation can be carried out at much lower pressures. This fact is associated with a reduction of the radioactive inventory as well as an improvement in process safety.

3. Optimization of fixation conditions

Three diferent autoclaves were employed in this work:

a) 50 liter cold wall autoclave having a usefull volume of < 4 liter, designed for 1000 bar and 1500 ^{o}C (see Fig. 1)

b) a battery of four outside heated autoclaves with 10 cm^3 inner volume, designed for 7000 bar and 750 ^{o}C. Each autoclave is provided with a pressure sensor and several thermoelements both inside and outside of the autoclave (see Fig. 2)

c) an outside heated autoclave with 10 cm^3 inner volume, designed for 700 ^{o}C and 1000 bar. The seal head of this autoclave is located inside the oven. Three thermoelements inside the autoclave are employed to measure the temperature. The oven is characterized by a very low heat loss.

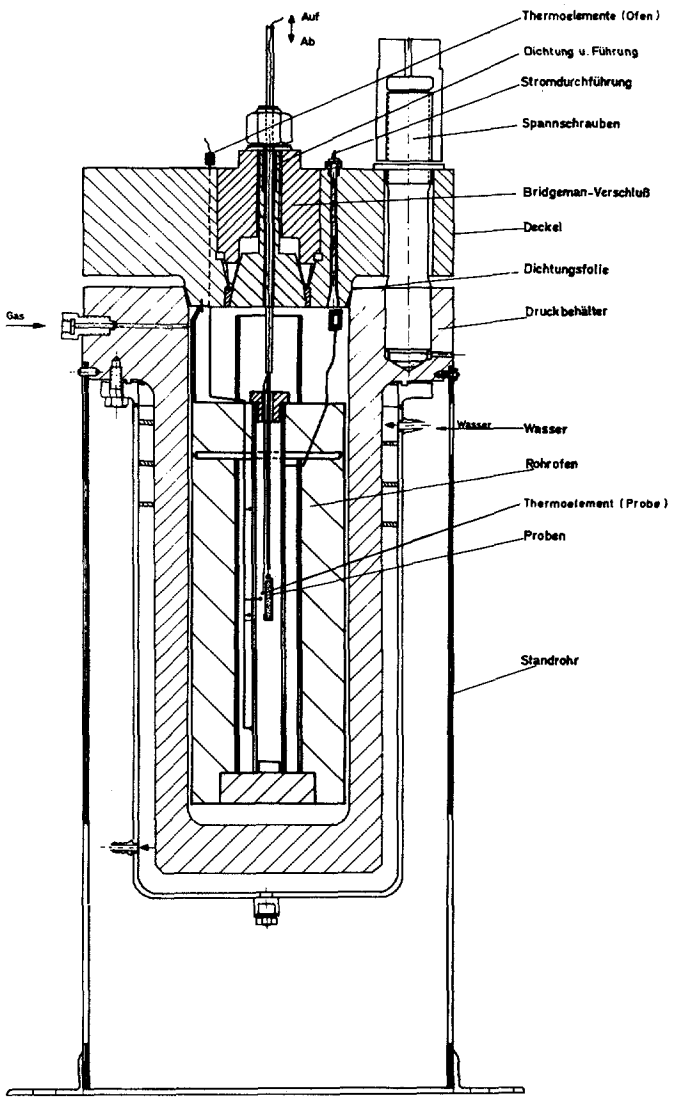

Fig. 1 50 liter cold wall autoclave.

Fig. 2 battery of four autoclaves

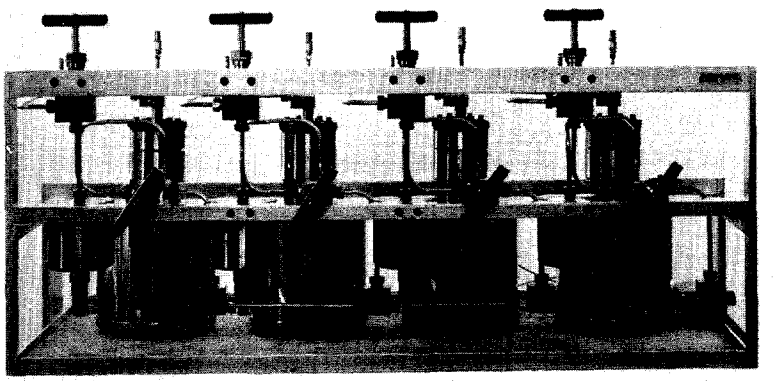

Unless otherwise specified, the samples were pretreated at temperatures between 200 and 400 °C for about 24 hours, quickly introduced into the autoclave, evacuated at more than 150 °C and loaded with noble gas for about 4 hours.

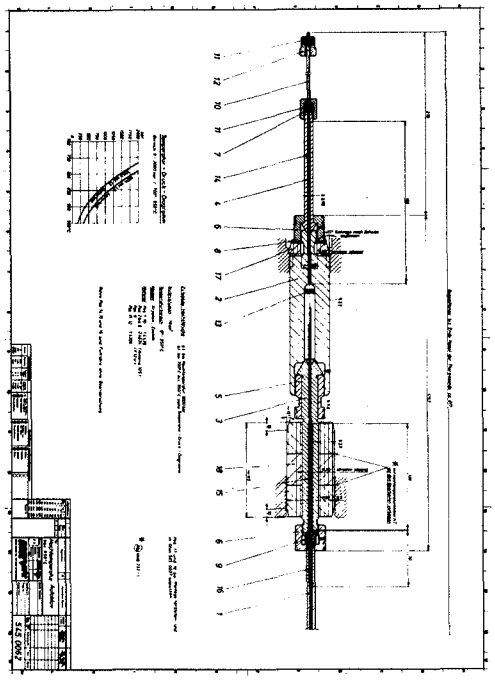

Fig. 3 10 cm^3 autoclave with three thermoelements .

3.1 Optimization of the fixation temperature

In two series of runs with a Sr 5A (15 % by weight of SrO) zeolite and a Ca 5A (15 % by weight CaO) zeolite the krypton loading was determined as a function of temperature. The experiments were carried out with autoclave c) positioned in a highly temperature stable oven, whose temperature could be kept constant to ± 10 °C. The fixation temperature was measured at the center line of the zeolite matrix with three thermoelements positioned near the bottom, the center and the upper part of the autoclave. During encapsulation (400 - 550 °C) the temperature of the oven was about 25 °C higher than those in the autoclave, the latter agreeing between each other to ± 7 °C. The results obtained with samples pretreated for at least 16 h at 200 °C and loaded at approximately 2000 bar Kr, are shown in Fig. 4 (at these pretreatment conditions only about 90 % of the crystalisation water is removed).From the data it is apparent that temperatures above 440 °C are required for diffusion of noble gas atoms into the small β - cages of the zeolite framework (see Fig. 5) to occur at a significant rate. The highest loading for both samples was obtained in the temperature range 500 - 530 °C. At temperatures above these values equilibrium is apparently reached in the sorption time allowed, and thus the volume sorbed decreases with increasing temperature.

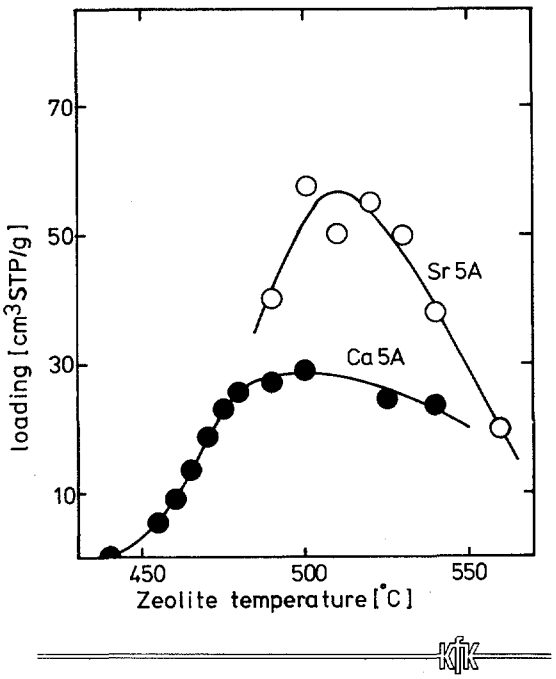

Fig. 4 Fixation of Kr (in cm^3STP/g) in Sr 5 A and Ca 5 A as a function of temperature (p=2000 bar, zeolite type NK202)

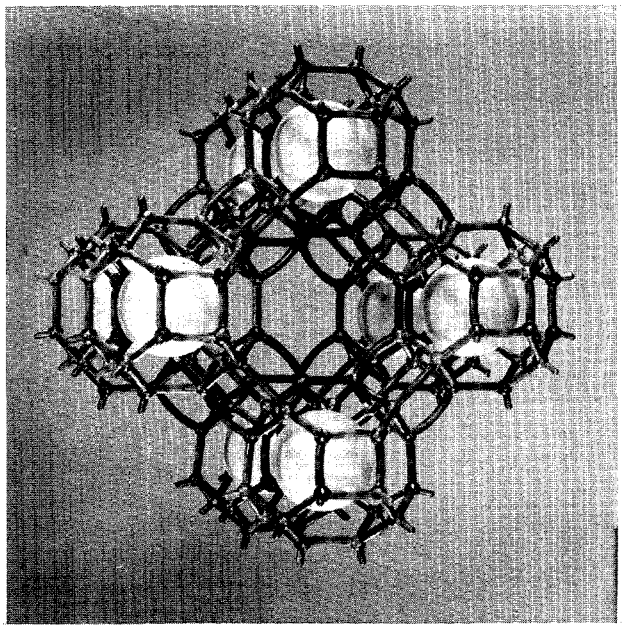

Fig. 5 Model of a 5 A zeolite showing a large empty α-cage and 8 small ß-cages, each occupied by a krypton atom.

3.2 Optimization of krypton loading by cationic exchange.

In an attempt to further reduce the pressure required for the fixation of Kr-85, type A zeolites, with known cationic composition, were systematically prepared and loaded with Ar, Kr and Xe under comparable conditions. Cationic exchange with K, Mg, Ca, Sr and Ba was carried out on a Bayer Na 4 A zeolite. Data on the cationic composition of the synthesized zeolites are summarized in Table I. In addition a number of commercial zeolites, whose chemical composition is given in Table II, as well as four NK 202 zeolites, having 15 % by weight of MgO, CaO, SrO and BaO, were investigated.

Fig. 6 shows some data on the dependance of Kr loading from the degree of cationic exchange, when the fixation is carried out at 2000 bar noble gas and 520 °C. It is seen that regardless of the degree of K exchange, no loading above 10 cm^3STP Kr/g

Table I Chemical data of cationic exchanged zeolites.

$\frac{MgO}{Al_2O_3}$	$\frac{CaO}{Al_2O_3}$	$\frac{SrO}{Al_2O_3}$	$\frac{BaO}{Al_2O_3}$	$\frac{K_2O}{Al_2O_3}$
0,13	0,102	0,12	0,10	0,167
0,24	0,298	0,29	0,19	0,284
0,36	0,466	0,42	0,30	0,369
0,52	0,683	0,58		0,569
0,64	0,910	0,77		0,863
0,78				

Table II Chemical composition of some commercial 5 A zeolites (in weight %)

Zeolite	SiO_2	Al_2O_3	CaO	Na_2O	MgO	K_2O
Roth 5 A	41.3	29.6 $\pm$ 2.3	11.5 $\pm$ 0.05	7.9	1.6	0.1
Bayer K 154	35.4	29.7 $\pm$ 2.3	12.9 $\pm$ 0.1	5.1	0.5	0.1
Ceca NK 202	42.5	27.1 $\pm$ 1.7	9.6 $\pm$ 0.1	6.2	2.2	0.3
Rhone-Poulenc	43.1	33.2 $\pm$ 1.5	10.8 $\pm$ 0.05	5.4	0.1	0.1

zeolite can be achieved. When,on the other hand, Ca exchanged samples are examined under similar conditions , higher loadings are obtained at all degrees of exchange. Furthermore, at $CaO/Al_2O_3 > 0.5$ the loading rises sharply reaching a maximum at about 0.7.

In another series of experiments Mg and Sr exchanged type A samples were loaded with Xe and Kr at p = 2000 bar and T = 793 K. Whereas the fixation of Kr and Xe is relatively insensitive to the degree of Mg exchange, the encapsulation of Xe

markedly decreases upon exchange with Sr (see Fig. 7). Not shown in Fig. 7 are

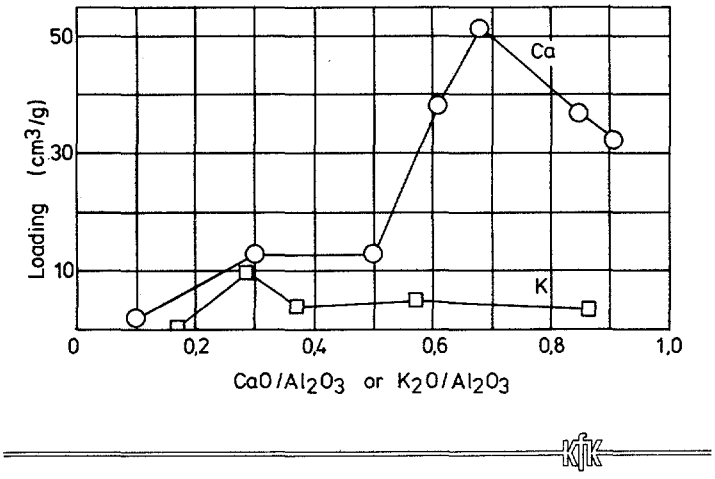

Fig.6 Kr loading as a function of K and Ca exchange of zeolite 4A (p = 2000 bar, T = 793 K)

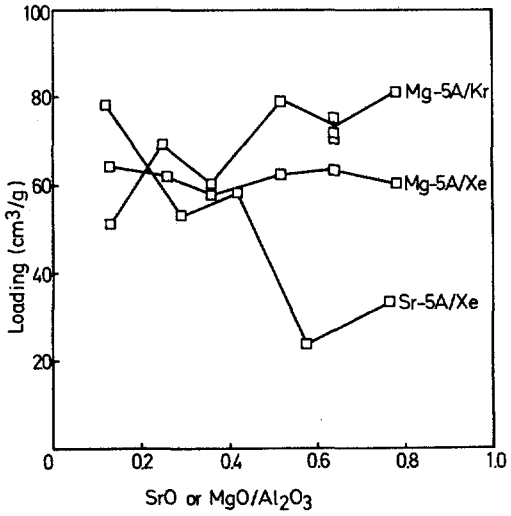

Fig. 7 Kr and Xe loading as a function of the Sr and Mg exchange (p = 2000 bar, T = 793, zeolite type A)

experiments on the fixation of Kr in Sr A zeolites. In this case a rather uniform increase in loading with increase in Sr exchange was observed, the maximum loading (approx. 62 cm^3STP/g)being reached at $SrO/Al_2O_3 \cong 0.6$. A few runs were also carried out with Ba substituted zeolites. As opposed to Mg, Ca and Sr exchanged molecular sieves they were found to be inadequate at the employed conditions for the conditionig of Kr, because Ba 5 A begins to decompose at relatively low temperatures ($\rangle$ 200 °C).

Experiments on the fixation of Ar in a large number of different zeolites have been reported previously 2/. Some additional results are compiled, together with data on Kr and Xe, in Table III. Clearly the extent of loading is highly dependent upon the type of gas being encapsulated.

It is difficult to rationalize these results without further information. Several, partly opposed effects, may play a significant role:

Table III Encapsulation of Ar, Kr and Xe in zeolites of type 5 A exchanged with several divalent cationic ions.

Zeolite M 5A (MO 15 % by weight)	Ionic crystal radius of M nm	Loading cm^3 STP / g Ar 1000 bar	Kr 2000 bar	Xe 2000 bar
Mg	0.066	-	72	63.5
Ca	0.099	27.3	43.9	-
Sr	0.115	16.9	70	27
Ba	0.137	7.7	1	-

- decrease in the number of cations in the α cages due to the progressing replacement of monovalent cations (Na) by divalent cations (increase of the effective free volume available for fixation).

- at some stage, after progressing exchange with a divalent cation, glassification sets in. This effect is of particular importance since it involves considerable additional trapping of noble gas in the large α cages (see Fig. 5)

- the characteristic potential energy of interaction between the different species to be encapsulated and the crystal,

- the kinetics of sorption, etc.

A monolithic rod prepared from Mg A zeolite (MgO/Al_2O_3 = 0.78) could be loaded within 4 h with about 18 % less Kr than 2 mm spheres. Since the density of the rod (ρ = 1.5 g/cm^3) is about twice as high as that of the spheres (bulk ρ = 0.7 g/cm^3), a considerable increase in loading as well as a substantial decrease of Kr-85 inventory during fixation seems possible simply by pressing the spheres into a rod. Further work on all these aspects as well as on the fixation of other potential impurities expected in the process gas after Kr-85 recovery from the off gas of a reprocessing plant is in progress.

3.3 Optimization of the fixation pressure.

Some typical sorption isotherms for Kr in zeolites exchanged with Mg, Ca and Sr are shown in Fig. 8 and 9. Even though in the high pressure limit higher loadings were

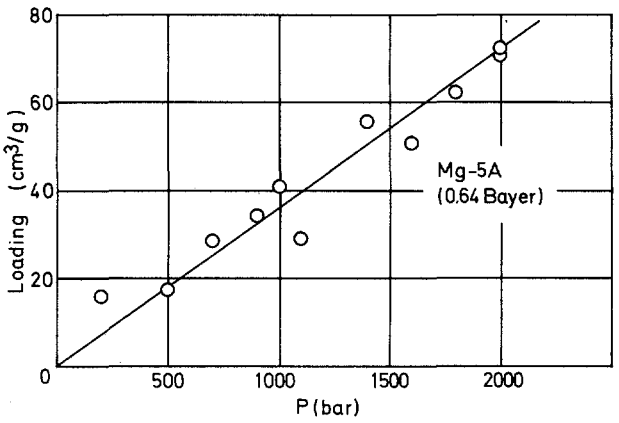

Fig.8 Sorption isotherm (T = 793 K) of Kr in Mg 5 A.

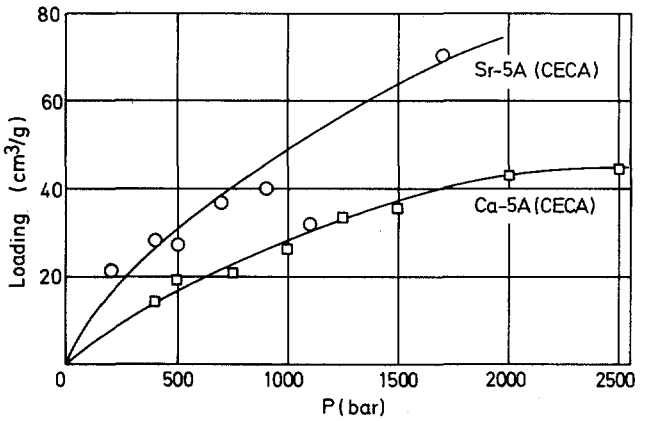

Fig. 9 Sorption isotherm (T = 793 K) of Kr in Ca 5A and Sr 5A.

obtained with Mg exchanged samples, the sorption kinetics into Sr 5A in the low pressure region is faster. The above data indicate that at 500 bar (from the point of view of long-term Kr-85 storage a loading of the order of 30 $\pm$ 10 cm^3STP/g is considered to be adequate) considerably more Kr can be encapsulated into CECA Sr 5A than into Bayer Mg 5A.Considerations of this kind are of importance to an improvement of safety for the encapsulation process.

4 Stability towards elevated temperature and radiation.

In previous work it was shown that no significant leackage of Kr occurs from zeolite Ca 5A samples containing between 19 and 57 cm^3STP/Kr/g kept at 200 ^{o}C for up to 2500 h or at 400 ^{o}C for up to 3500 h 2/. Similarly, a Sr 5A zeolite (15 % by weight SrO) loaded with 74.8 cm^3 STP Kr /g could be stored in an oven at 450^{o}C without significant loss of trapped gas. This result was confirmed in experiments with the same samples placed in a quartz tube provided with a break seal. From an analysis of the gas phase it was observed that at 450 ^{o}C, but also at room temperature, a small fraction of the encapsulated gas (about 0.03 %) is readily liberated within

hours.It appears that this leackage is mainly due to superficially adsorbed gas, because the initial gas liberation is not followed by an additional desorption.

In another desorption study, carried out in a gas flow system coupled to a automatic gas chromatograph, the sample was placed in a stainless steel tube and subjected to various temperature programms.The leackage, which could be plotted according to the Q_t/Q_∞ vs. $\sqrt{t}$ law 2/, yielded an activation energy for the decapsulation of Kr from Ca 5A of 209 kJ/mol (loading between 22,7 and 40.8 cm^3STP Kr/g) (see Fig.10).

Ca 5A zeolite, loaded with 34.8 cm^3STP Kr/g, looses almost completely its ability to adsorb water as well as other gases. For instance,whereas dried unloaded zeolite 5A shows at 20 °C a weight increase of about 4 % when exposed to a H_2O pressure 5.3 x 10^{-3} mbar after loading with Kr, a H_2O pressure nearly 400 times as high (≈ 20 mbar) is needed to bring about a weight increase of only 0.7 %.

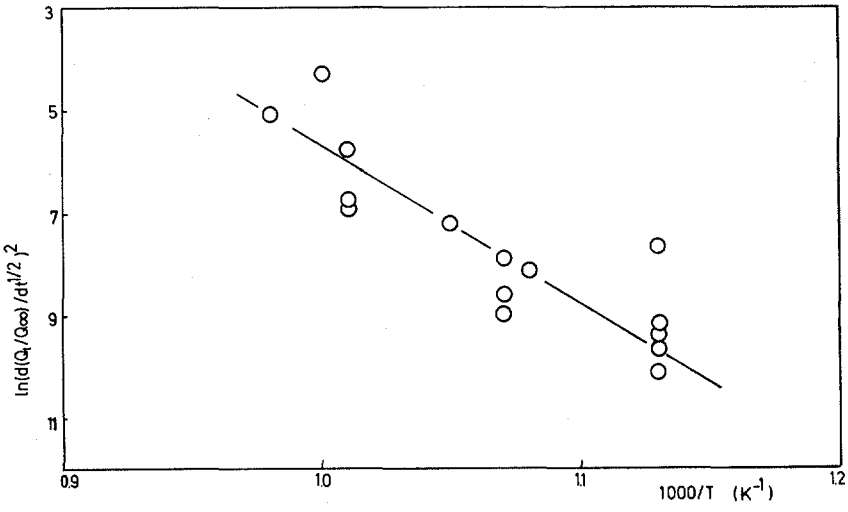

Fig. 10 Activation energy for Kr desorption out of Ca 5A.

There are indications that the extrem stability of the encapsulated gas towards elevated temperatures is due to some sort of glassification or sintering. As apparent from Fig. 11, the characteristic X ray pattern is lost when the zeolite Mg 5A is loaded with noble gas. Since the zeolite becomes amorphous irrespective of the degree of loading, it is clear that "highly stable" fixation can also be carried out at rel. low pressures, i.e. 200 bar. Fig. 12 shows that, in addition to Mg exchanged zeolites, also zeolites exchanged with Ca, Sr or Ba become amorphous after noble gas sorption.

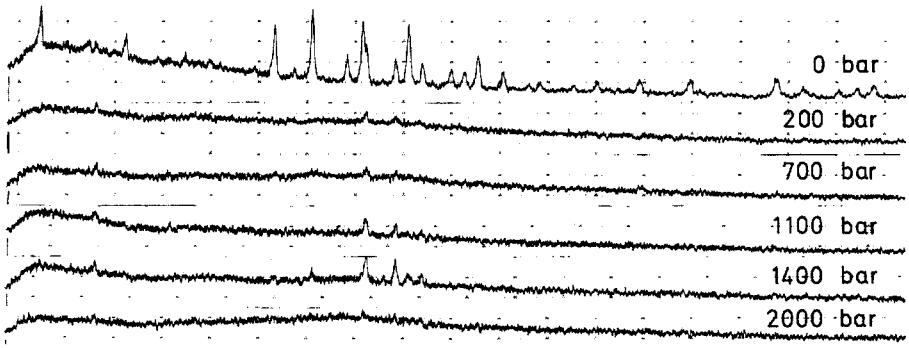

Fig. 11 X-ray analysis of Mg 5A (MgO/Al_2O_3 = 0.64) zeolite after loading at various pressures.

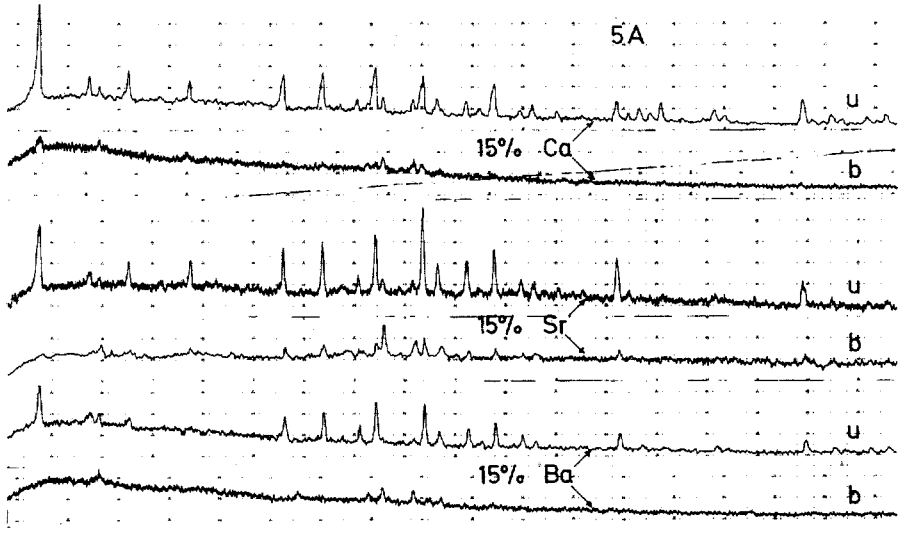

Fig. 12 X-ray analysis of unloaded (u) and Kr loaded (b) Ca, Sr and Ba 5A zeolite.

The effect of radiation from encapsulated Kr-85 was simulated by irradiating 2 g of NK 202 Sr 5A zeolite loaded with 59.8 cm^3 STP Kr/g with six burned fuel elements placed in a water pool.From four samples irradiated with increasing γ-ray dosis, only three have been analysed and compared with an unirradiated sample.The results, summarized in Table IV, suggest that radioactive radiation does not lead to a significant liberation of gas.Future experimental work will involve the encapsulation of Kr-85. Small samples with the specific activity expected during final Kr-85 storage will be prepared.

With a 10 cm^3 autoclave coupled to a 40 cm^3 Cu/Be cryogenic vessel, it was demonstrated that the fixation of Kr can be carried out without the emploment of me-

Table IV Effect of radioactive radiation.

Energy dosis (rad)	% Kr liberated
0	0.023
0.33×10^8	0.035
1.03×10^8	0.029
3.02×10^8	0.033

canical compression. Two Kr sources were used:either a steel cylinder pressurized with 80 bar or a 23 liter glass vessel containing 1 bar.To encapsulate,the gas was first frozen out into the cryogenic vessel. Then the cryogenic vessel was isolated with a valve and the solidified gas expanded into the cryogenic container as well as into the previously evacuated autoclave containing the zeolite. After a pressure of about 190 bar was reached in the autoclave, the latter was isolated with a valve, heated to 793 K and kept at that temperature for about 4 h (p = 500 bar). Once the encapsulation was completed, the non trapped gas could be frozen back into the cryogenic vessel.

An engineering study on the encapsulation of Kr-85 in zeolites is presently in progress.

Acknowledgements: The technical assistance of P. Schuster, F. Bauer and U. Berndt is gratefully acknowledged. The synthesis of special zeolites by L. Puppe is also acknowledged with gratitude.

Literatur

1/ Benedict R.W.,Christensen A.B.,Del Debbio J.A., Keller J.H. and Knecht D.A. Technical and Economical Feasibility of Zeolite Encapsulation for Kr-85 Storage ENICO-Report Nr. 1011, Sept. (1979)

2/ Penzhorn R.-D., Schuster P.,Noppel H.E. and Hellwig L.M. Long-term Storage of Kr-85 in Zeolites. Int. Symp. on Management of Gaseous Wastes from Nuclear Facilities, Vienna, Feb. (1980)

DISCUSSION

ORTH: What is the influence on the loading characteristics of krypton of the presence of large amounts of other gases, such as nitrogen?

PENZHORN: We have not done experiments on mixtures of gases. We have, however, shown that argon, krypton, and xenon can be encapsulated. I would suspect that other gases, depending on their kinetic diameter, can also be encapsulated in zeolite 5A. Experiments to determine specific fixation rates should be carried out.

D. KNECHT: I would just like to comment that we have been encapsulating krypton in zeolite 5A since Dr. Penzhorn informed us of his work last spring, and we are getting similar results. We do not have the temperature, or the sensitivity to temperature, that he has, so we cannot say whether we have the same temperatures. We are getting loadings in the range of 40-60 cc/g at 1,000 BAR and around 600-700°C.

TINGEY: Some of you may not be aware that we reported similar work using silica to trap krypton a year ago in Boston and again in Vienna. We used a porous silica glass with about 30% porosity, which was loaded with krypton at high pressures and then sintered at 900°C. The krypton loaded glasses are stable to temperatures of 800-900°C. The Kr loadings are dependent upon pressure, and are in the range of 20-40cc (STP) of Kr/cc of glass for loading pressures above 35 MPa.

PENZHORN: I think there is still one very important experiment that needs to be carried out. It is in preparation in Karlsruhe. It involves the encapsulation of krypton-85. We should show that rubidium, produced inside the cage system, will not affect the leakage rate.

LONG-TERM STORAGE OF RADIOACTIVE KRYPTON USING ADSORBENT AND A DOUBLE CYLINDER

Y. Yamamoto, Y. Sawada, B. An
Kobe Steel, Ltd., Kobe, Japan
and
E. Inada
Power Reactor and Nuclear Fuel
Development Corp., Tokai, Japan

Abstract

Long-term storage of krypton gas is important from the viewpoint of reducing the release of radioactivity to the atmosphere. The storing method using adsorbent is anticipated to be brought into practical use as an intermediate storing method before the final disposal and/or storage technology of krypton gas is established.

The concept of remote-controlled storage system for krypton has been studied and clarified with a process involving a double cylinder and adsorbent. Experimental studies on adsorption and heat transfer characteristics of adsorbent and storage gas systems have also been performed. When stored, the temperature inside the cylinder increases due to the decay heat of krypton-85. Then a part of the krypton adsorbed on the adsorbent is desorbed and the pressure inside the cylinder is apt to rise. However, from the experimental and analytical studies, the capability of storage at a lower pressure inside the cylinder by dint of the adsorbing effect compared with the pressure without adsorbent was confirmed.

I. Introduction

A large amount of krypton gas is to be recovered from reprocessing plants. Enthusiastic researches are being carried out on long-term storage techniques of krypton such as high pressure cylinder storage[1],[2], zeolite encapsulation[3],[4], ion-implantation and so on[5]. The storing method using adsorbent is well known and anticipated to be brought into practical use as an intermediate storing method before the final disposal and/or storage technology is positively established.

In the storage system, storage gas is charged into the inner cylinder at low temperature and stored for a long time at room temperature after the outer cylinder is sealed off by welding. For the purpose of estimating the temperature and pressure inside the cylinder at the time of storage, adsorption and heat transfer characteristics of adsorbent and storage gas systems have been studied. Activated charcoal has been used as adsorbent on the basis of previous studies.

In this paper, the concept of remote-controlled storage system and the results of experimental and analytical studies on adsorption and heat transfer characteristics are described.

II. System Description

System Flow

In the storage system, storage gas is first charged into the inner cylinder by dint of the adsorbing effect of adsorbent at low temperature. The cylinder filled with storage gas is stored for a long time at room temperature after the outer cylinder is sealed off by welding. The double cylinder is air-cooled at the time of storage. The amount of storage gas charged in one double cylinder is set at 1.2×10^5 Ci, as shown in Table I.

Table I Storage gas charged in one cylinder

Gas Volume	1,100 Nl
Radioactivity	1.2×10^5 Ci (^{85}Kr)
Heat Generation	148 kcal/hr
Composition	Kr $\geqq$ 90%
	N_2 $\leqq$ 10%

A schematic flow sheet of the system is shown in Figure 1. The double cylinder is prepared and set on a cart in such a way that the inner cylinder is filled with regenerated adsorbent and the outer cylinder is un-welded. In this step, necessary operations are done directly because the process is free from radiation exposure, while in the subsequent steps all operations are remote-controlled. Then, the pipe for feeding storage gas is connected to a pipe connector attached to the inner cylinder, and the valve is opened. The double cylinder is cooled by liquid nitrogen, and the storage gas is automatically charged into the inner cylinder by dint of the adsorbing effect of adsorbent at low temperature below atmospheric pressure.

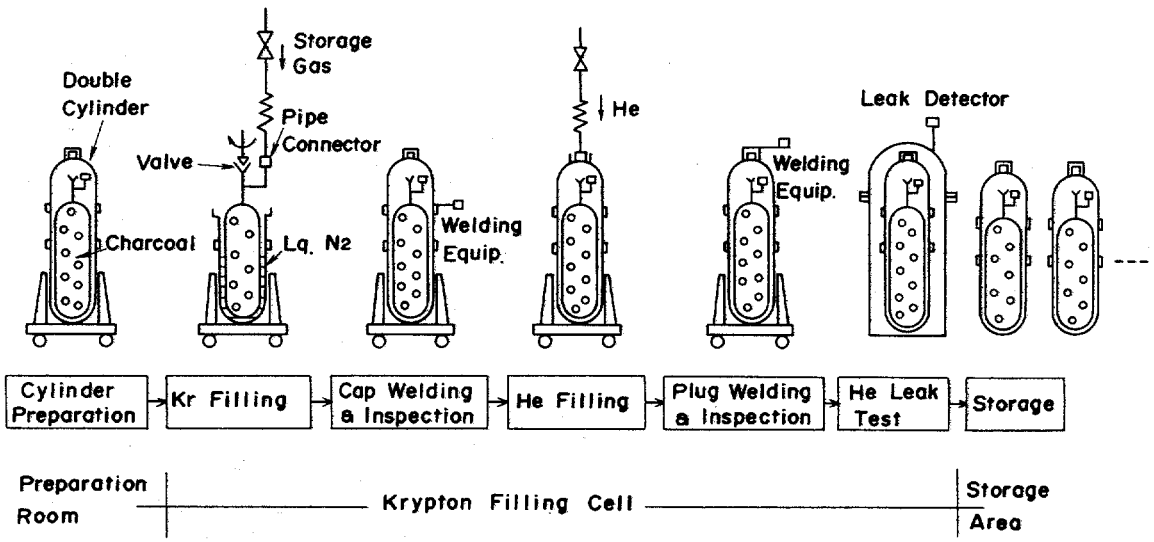

Figure 1 Schematic flow sheet of the krypton storage system

After it is confirmed that the storage gas has been sufficiently transferred to the inner cylinder, the valve is closed and the pipe connector is detached. Pipe connection and valve operation are done

by specially designed robots. As for these robots, actual scale models were fabricated for trial and the function has now been verified. Then, the head of the outer cylinder is TIG-welded, and the gap between the inner and outer cylinder is filled with helium. Filling up with helium is intended both to improve the heat transfer characteristics of the double cylinder and to perform helium leak test to confirm the soundness of welded parts. Then the double cylinder is finally inspected by helium leak test after the plug used in helium charging is TIG-welded and is stored for a long time in the storage area.

It is one of the features of the system that storage gas can be charged into cylinders below atmospheric pressure without using a compressor. It is also noticeable that the system is easily remote-controlled, and the radioactivity released to the atmosphere is negligible. The pressure inside the cylinder at the time of storage is very low compared with that of high pressure cylinder storage and the cylinder is double structual, then the possibility of radio-activity release from the cylinder is small. Consequently, the storage facility could be simplified. Storage gas will easily be retrieved when the final disposal and/or storage technology is positively established in the future.

Double Cylinder

The double cylinder has good heat transfer characteristics in order that the heat generated due to decay of krypton is efficiently transferred to the outside and is shown in Figure 2.

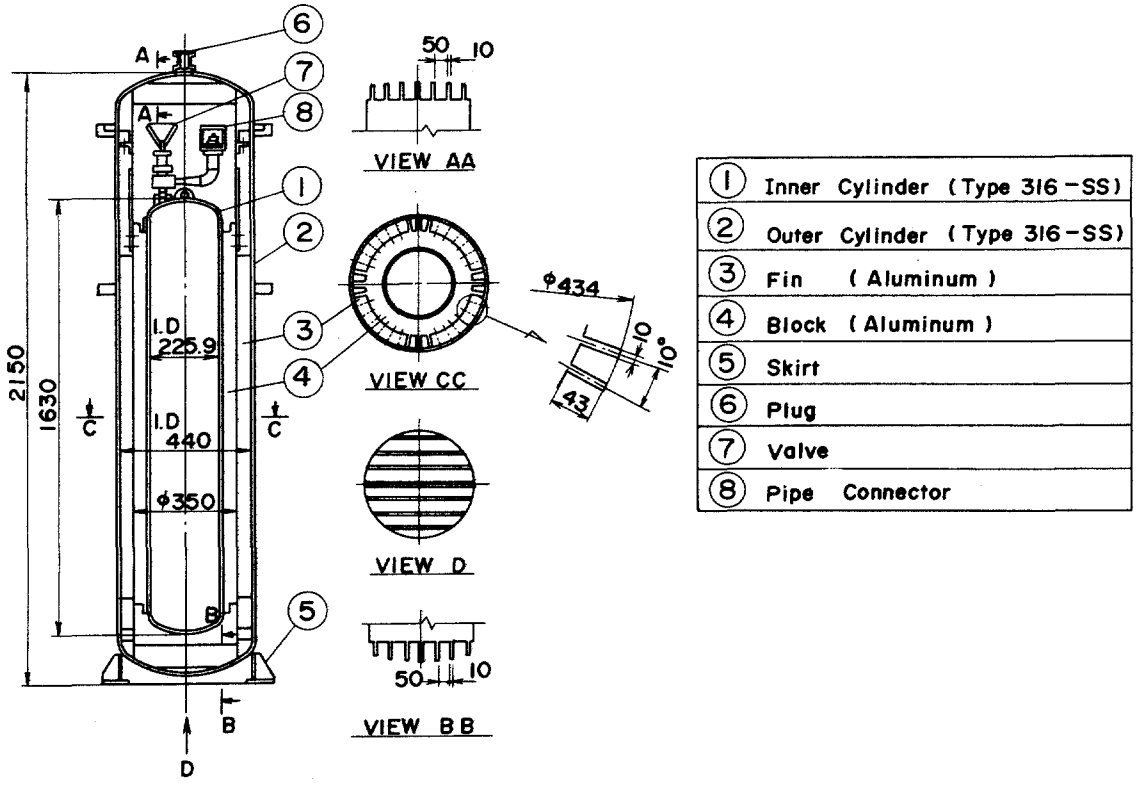

Figure 2 Double cylinder for krypton storage

The difference of temperature between the outer and inner cylinder is 10°C in steady state conditions as a design base. The double cylinder has such a structure that the inner cylinder will be protected in case of drop from maximum height of three meters, assuming mishandling.

The double cylinder consists of inner and outer cylinder made of stainless steel. Aluminum shock absorbers which excel in heat transfer and shock absorbing properties are equipped in the space between the inner and outer cylinder. The inner cylinder is filled with charcoal, Kurare-4GA, of which properties are shown in Table II. The inner cylinder is placed on shock absorber provided in the bottom of the outer cylinder and is also surrounded with shock absorber. In the upper part of the inner cylinder, a pipe connector and valve are attached, which are designed to be operated easily by robots and are also protected with aluminum blocks. The space between the inner and outer cylinder is filled with helium at the pressure of 1 atm through the plug attached the upper part of the outer cylinder. A skirt is provided in the lower part of the outer cylinder so that the cylinder stands by itself.

Table II Properties of charcoal (Kurare-4GA)

Bulk Density	0.55 g/cm^3
Absolute Density	2.1 g/cm^3
Ash	1.8 %
Pellet Size	4 mmϕ × 7 mm^L
Void Fraction	0.4

The heat transfer experiments with an actual scale double cylinder shown in Figure 2 were carried out. The experimental results agreed fairly well with the finite differential analysis using TRUMP Code and showed that the design base mentioned above was satisfied. When the double cylinder is dropped from a hight of 3 meters, it was confirmed that the potential energy is absorbed by the aluminum shock absorber so that the inner cylinder will be protected by the structural analysis.

III. Experimental

Apparatus

The apparatus for adsorption and heat transfer experiments is shown in Figure 3. The cylinder is made of stainless steel with the capacity of 5.7 liters. The maximum pressure in the cylinder is 40 kg/cm^2 and the temperature is optionally controlled by the heaters provided in the center and outside of the cylinder. The cylinder is filled up with charcoal shown in Table II, and temperatures at each position are measured by C-A thermocouples. Heat flux in the radial direction is measured by heat flux meter. An optional amount of gas can be supplied to the cylinder and evacuated through oil diffusion pump and rotary pump. The cylinder is fabricated in leaktight structure, using copper gaskets.

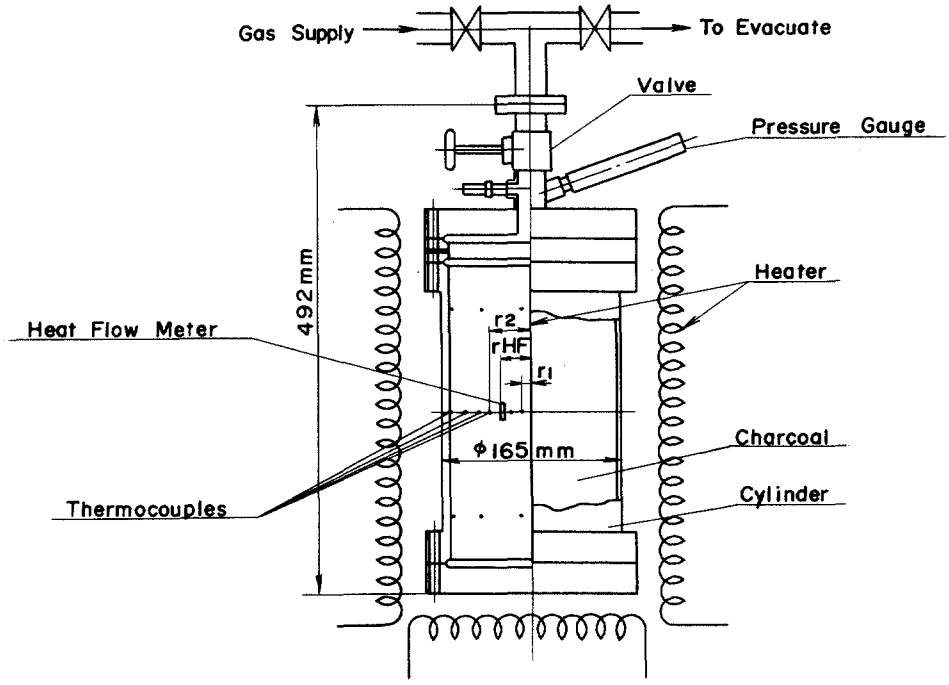

Figure 3 Apparatus for adsorption and heat transfer experiments

Procedure

Charcoal is regenerated for about 4 hours at a temperature of about 200°C and a pressure of 10^{-2} to 10^{-3} Torr. The cylinder is cooled by liquid nitrogen and an optionally fixed amount of feed gas is adsorbed on charcoal in the cylinder. The temperature of the cylinder and charcoal are uniformly elevated to a specified value by the heaters, and the pressure is measured. The amount of gas adsorbed on one gram of charcoal is computed by means of making balance of the gas amount which was fed and exists in the space inside the cylinder. Then the heater outside the cylinder is turned off and heated only by the heater located in the center of the cylinder, and the temperature and heat flux at each position are measured until the steady state conditions are attained. According to the measured temperature and heat flux, the effective thermal conductivities of the system consisting of charcoal and feed gas are calculated in the equation as follows, assuming the system is infinite cylinder.

$$k = \frac{r_{HF}\, q \ln r_2/r_1}{T_1 - T_2} \qquad (1)$$

where, k = effective thermal conductivity, kcal/mhr°K

q = heat flux at $r = r_{HF}$m, kcal/m^{2}hr

$T_{1,2}$ = temperature of thermocouples at $r = r_1$m and $r = r_2$m, °K

IV. Experimental Results and Discussion

Adsorption Studies

The greater part of storage gas as presented in Table I is krypton with a maximum content of 10% nitrogen. Adsorption characteristics were experimentally studied in three kinds of gas, 100% krypton, 100% nitrogen, and 90% krypton-10% nitrogen mixture. Adsorption isotherms of krypton charcoal, nitrogen-charcoal, and mixed gas-charcoal systems were obtained, and shown in Figures 4, 5 and 6, respectively. In the adsorption isotherms shown in these figures, it is noticeable that the adsorbed amount, in all cases, increased linearly with pressure, passing the origin, which suggests the adsorption characteristic of Henry type. According to these figures, the adsorbed amount, x in STP cc/g, per one gram of charcoal is expressed as follows, using pressure, P in atm and constant K(T) which is a function of temperature, T in °K:

$$x_{Kr} = K_{Kr}\ (T)\ P_{Kr} \tag{2}$$

$$x_{N_2} = K_{N_2}\ (T)\ P_{N_2} \tag{3}$$

$$x^{ex}_{Kr+N_2} = K^{ex}_{Kr+N_2}\ (T)\ P_{Kr+N_2} \tag{4}$$

where $x^{ex}_{Kr+N_2}$ and P_{Kr+N_2} are the total amount adsorbed and the pressure of krypton and nitrogen. These experimentally obtained values will be compared with the calculated values. The gradient K(T) of each adsorption isotherm is obtained by a least square linear regression analysis, and plotted against the reciprocal temperature in Figure 7. K(T) shown in Figure 7 is also fitted by equations of the form expressed as follows, which are very convenient ones for the design use.

$$x_{Kr} = 5.2 \times 10^{-2}\ P_{Kr}\ \exp\frac{3.7}{RT} \tag{5}$$

$$x_{N_2} = 7.4 \times 10^{-2}\ P_{N_2}\ \exp\frac{2.7}{RT} \tag{6}$$

$$x^{ex}_{Kr+N_2} = 6.4 \times 10^{-2}\ P_{Kr+N_2}\ \exp\frac{3.3}{RT} \tag{7}$$

where R is the gas constant in kcal/mol°K.

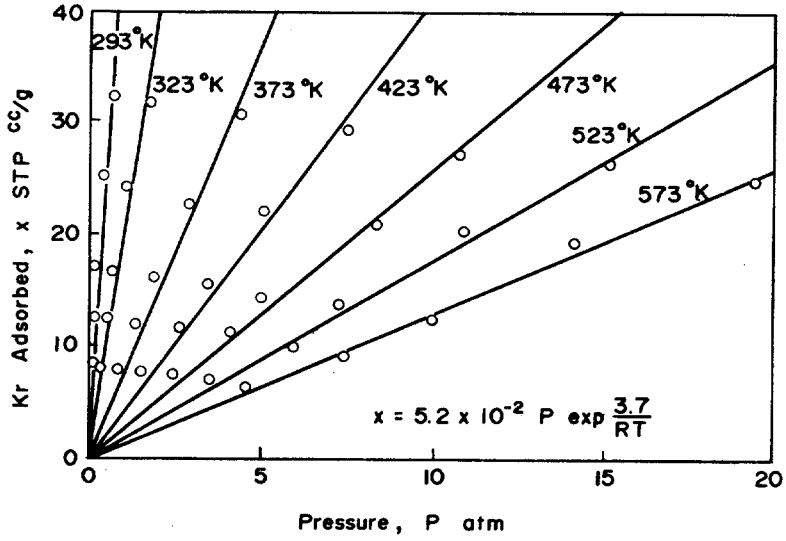

Figure 4 Adsorption isotherms for Kr-charcoal system

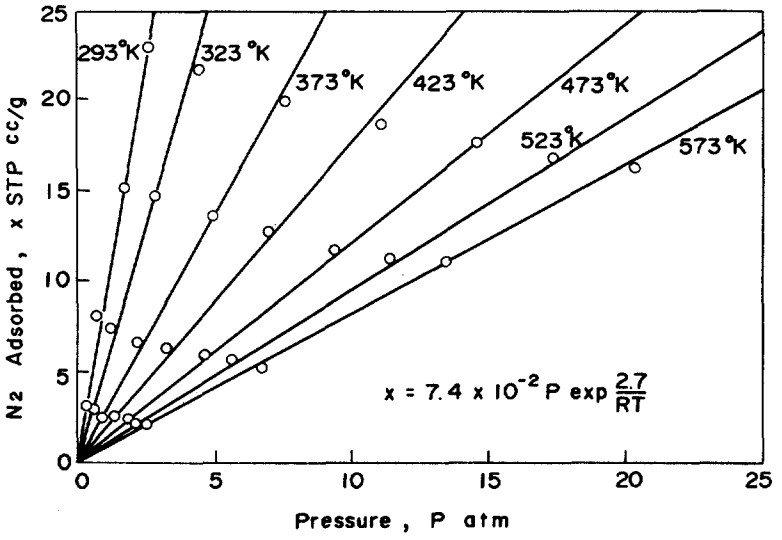

Figure 5 Adsorption isotherms for N_2-charcoal system

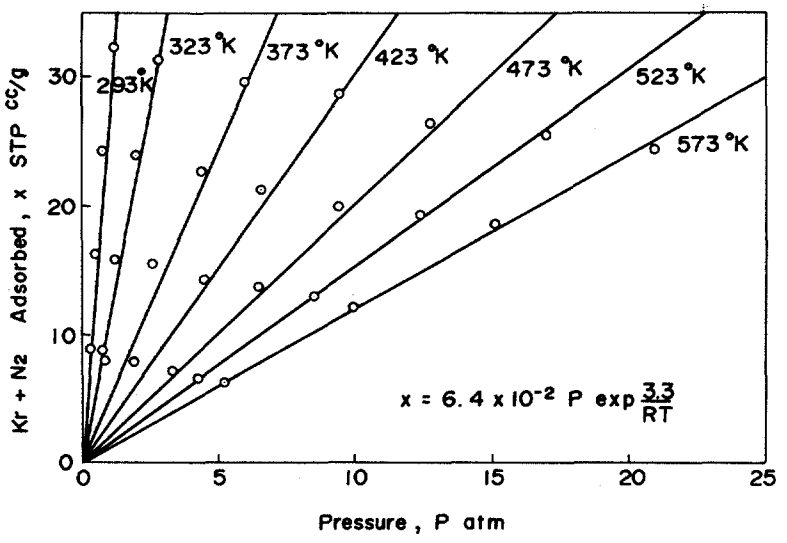

Figure 6 Adsorption isotherms for $Kr+N_2$-charcoal system

As for the adsorption characteristics of the mixed gas of 90% krypton-10% nitrogen, the calculated amount of the mixed gas adsorbed $x^{cal}_{Kr+N_2}$ is given by equation (8) on the assumption that each component behaves independently of the other.

$$x^{cal}_{Kr+N_2} = x_{Kr} + x_{N_2} = K_{Kr}(T)P_{Kr} + K_{N_2}(T)P_{N_2} \quad (8)$$

where x_{Kr}, x_{N_2}, P_{Kr} and P_{N_2} refer to the amount adsorbed and the partial pressure of each gas. The amount of each component existing in unit volume, V_{Kr}, V_{N_2} is given respectively by equation (9) from the total of the amount adsorbed on charcoal and the amount existing in the space:

$$V_{Kr,N_2} = \frac{273P_{Kr,N_2}\,\varepsilon}{T} + \rho x_{Kr,N_2} \quad (9)$$

where ε = void fraction of charcoal
ρ = bulk density of charcoal

Since the system mentioned here is uniform, equation (10) is given from the composition of the mixed gas.

$$\frac{V_{N_2}}{V_{Kr}} = \frac{1}{9} \tag{10}$$

Then the calculated amount of mixed gas adsorbed is expressed by equation (11), being derived from equations (8), (9) and (10).

$$x^{cal}_{Kr+N_2} = \frac{9K_{Kr}(T)\kappa(T) + K_{N_2}(T)}{1 + 9\kappa(T)} (P_{Kr} + P_{N_2}) \tag{11}$$

$$= K^{cal}_{Kr+N_2} (P_{Kr} + P_{N_2})$$

where,

$$\kappa = \frac{\frac{273}{T}\varepsilon + \rho K_{N_2}(T)}{\frac{273}{T}\varepsilon + \rho K_{Kr}(T)} \tag{12}$$

Now, $x^{cal}_{Kr+N_2}$ is numerically computed from equation (11) using the experimentally obtained values of K_{Kr} and K_{N_2} and expressed as follows:

$$x^{cal}_{Kr+N_2} = 5.9 \times 10^{-2} (P_{Kr} + P_{N_2}) \exp \frac{3.5}{RT} \tag{13}$$

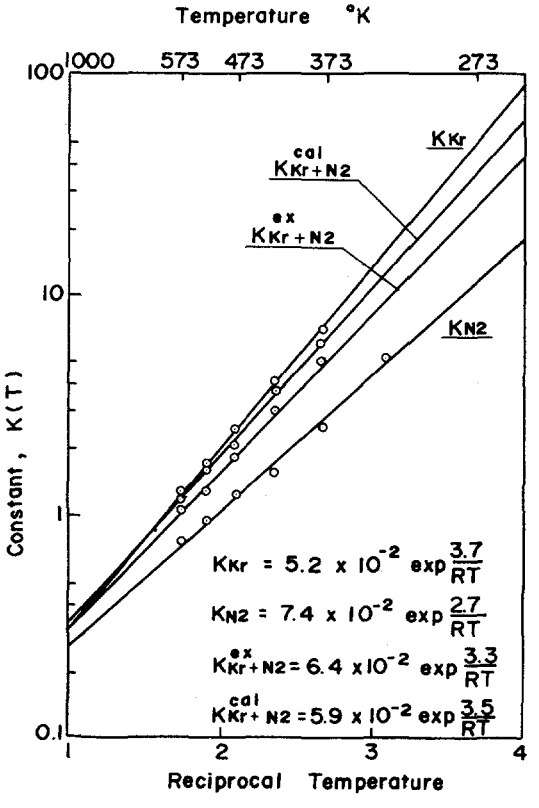

Figure 7 Plots of constant K(T) as a function of temperature

$K^{cal}_{Kr+N_2}$ is also plotted in Figure 7 and is compared with $K^{ex}_{Kr+N_2}$ in equation (7). The calculated values are 10 to 20 percent higher than the experimental values, which suggests that there exists some kinds of krypton-nitrogen interaction in the mixed gas-charcoal system.

Heat Transfer Sfudies

The effective thermal conductivities of the system consisting of krypton gas and charcoal were obtained by the procedure mentioned above, and are shown in Figure 8. Values of effective thermal conductivity tend to increase as the pressure and temperature increase, and all the measured values indicated around 0.1 kcal/mhr°C. To estimate the temperature and pressure inside the cylinder at the time of storage, the minimum measured value shown in Figure 8, which is 0.08 kcal/mhr°C, is used.

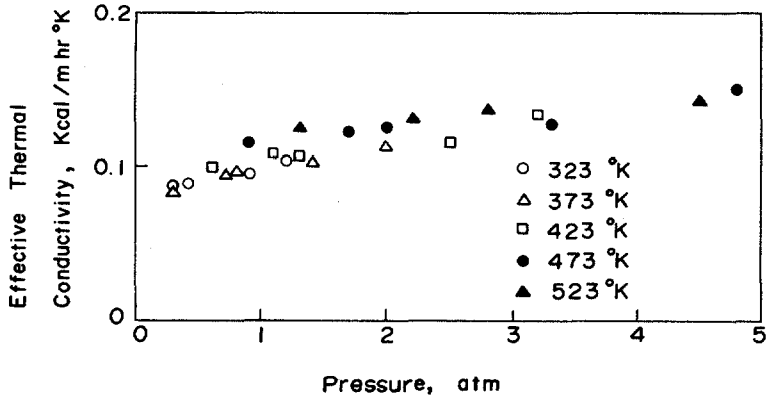

Figure 8 Effective thermal conductivities of Kr-charcoal system

Temperature and Pressure inside the Cylinder

The temperature and pressure inside the cylinder is discussed in the case that mixed gas of 90% krypton-10% nitrogen as presented in Table I is stored in a cylinder with the length of 2 meters. Assuming the cylinder is infinite, the steady-state heat transfer equation inside the cylinder is given by equation (14), which is derived from equations (7) and (9).

$$k \frac{d^2T}{dr^2} + k \frac{1}{r} \frac{dT}{dr} + \alpha P\left(\frac{273}{T}\varepsilon + 6.4 \times 10^{-2}\rho \exp\frac{3.3}{RT}\right) = 0 \qquad (14)$$

where,

T = temperature at a position of r meters from the center of the cylinder, °K.

α = heat generated per 1 Nm^3 of storage gas, kcal/Nm hr.

Heat generation Q in kcal/hr per unit length of the cylinder is given by

$$Q = \int_{r=0}^{r=r_o} \alpha P\left(\frac{273}{T}\varepsilon + 6.4 \times 10^{-2}\rho \exp\frac{3.3}{RT}\right) 2\pi r dr \qquad (15)$$

$$= 74$$

Equation (14) was dissolved by means of finite differential method using equation (15) and equations (16), (17) which are boundary conditions, and temperature and pressure inside cylinder were obtained.

$$T_{r=r_0} = Tr \tag{16}$$

$$\frac{dT}{dr}\Big|_{r=0} = 0 \tag{17}$$

where r_0 is the cylinder radius. As a result, the temperature distribution inside the cylinder in the steady state condition with the capacity of 60 liters was obtained, and is shown in Figure 9. For instance, in one case that the surface temperature of the cylinder is 333°K, the temperature in the center of the cylinder is about 400°K and the pressure is 4.3 atm. The relation of the capacity of the cylinder, cylinder surface temperature and pressure is compared with those without charcoal and is shown in Figure 10. The pressure inside the cylinder without charcoal is calculated on the assumption that the temperature of storage gas is equal to the cylinder temperature. For instance, when the cylinder capacity is 60 liters and surface temperature is 333°K, the pressure without charcoal is 22 atm, which is about 1/5 of that with charcoal mentioned above.

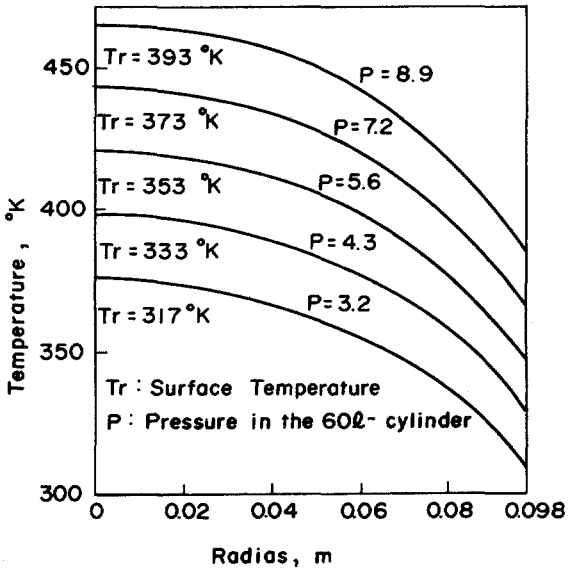

Figure 9 Temperature distribution inside the cylinder

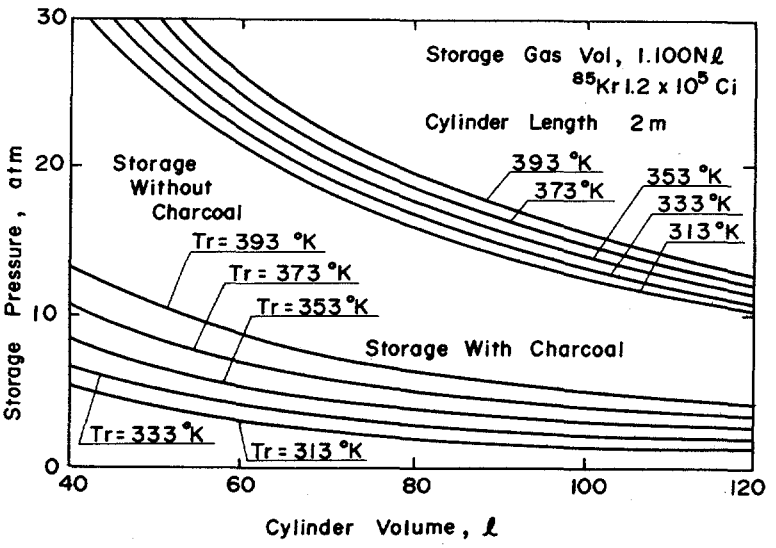

Figure 10 Relation between cylinder volume, storage pressure and temperature

V. Conclusion

1. The storage system of krypton gas with a process involving adsorbent and a double cylinder was clarified.

2. As a result of studies on the adsorption characteristics of the system consisting of storage gas and charcoal, adsorption data necessary for designing were obtained.

3. As a result of studies on the heat transfer characteristics of the system consisting of storage gas and charcoal, heat transfer data necessary for designing were obtained.

4. Methods of heat transfer and adsorption analysis inside the cylinder at the time of storage was considered, and the pressure inside the cylinder was estimated by using the experimental data.

5. The pressure inside the cylinder was confirmed to be rather low compared with that of high pressure cylinder storage.

Acknowledgement

This work was performed under contract with Power Reactor and Nuclear Fuel Development Corp. (PNC)

The authors wish to express their gratitude to Mr. N. Tsunoda and Mr. T. Horiuchi for profitable comments and discussion. Mr. S. Kusumoto is also gratefully acknowledged for his experimental assistance.

References

1. B. A. Foster and D. T. Pence, "An evaluation of high pressure steel cylinders for fission product noble gas storage," ICP-1044, Idaho National Engineering Laboratory, February 1975

2. R. A. Brown, D. A. Knecht and T. R. Thomas, "Reference facility description for the recovery of iodine, carbon and krypton from gaseous wastes," ICP-1126, Idaho National Engineering Laboratory, April 1978

3. R. A. Brown, M. Hoza and D. A. Knecht, "^{85}Kr storage by zeolite encapsulation", Proceedings of the 14th ERDA Air Cleaning Conference, CONF-760822, Vol. 1, p. 118, February 1977

4. R. W. Benedict, A. B. Christensen, J. A. Del Debbio, J. H. Keller, and D. A. Knecht, "Technical and economic feasibility of zeolite encapsulation for krypton-85 storage", ENICO-1011, Exxon Nuclear Idaho Company, September 1979

5. D. A. Knecht, "An evaluation of methods for immobilizing krypton-85", ICP-1125, Idaho National Engineering Laboratory, July 1977

DISCUSSION

RUTHVEN: Last year, Dr. Mack had a paper published about various varieties of steel, some of which showed damage because of the krypton-85 decay products. I wonder if you have taken into consideration what type of steel to use for the steel cylinders. Have you taken into account the corrosion damage caused by the medium on the steel cylinders when using particular types of steel?

YAMAMOTO: The decay product, rubidium, will be produced on a large surface area of charcoal. And very small amounts of rubidium would contact the cylinder material. Then we have to pay less attention to the material corrosion problem than the case of high-pressure cylinder storage. Stainless steel type-316L, to be used, is also one of the corrosion resistant materials.

DAVIS: What you mean, essentially, is that there will not be a significant amount of leakage from the adsorbent to the surface of the cylinders?

YAMAMOTO: Yes, very small amounts of rubidium would exist on the cylinder surface, because the surface area of charcoal is much larger.

EVANS: Have you considered the use of 5A storage medium in your cylinders rather than charcoal? It seems to me that this would have somewhat better properties with respect to potential heat resistance and also the ability to adsorb the rubidium that is formed by the decay of the krypton.

YAMAMOTO: I also carried out adsorption and heat transfer experiments on storage gas and some types of zeolite systems. According to them, adsorption characteristics of charcoal was considered most feasible.

PENZHORN: Aren't there other gases to be expected besides nitrogen? For instance, methane or some oxygen--wouldn't you take that into consideration, also? I would say that you can get as much as 100 g of rubidium from the decay of krypton-85.

YAMAMOTO: Storage gas would contain a small amount of argon, oxygen and other gases. Even if they react with charcoal, the reduction of the surface area wouldn't be serious. Then the pressure inside the cylinder wouldn't increase.

PENZHORN: When do you expect your plant to work under hot conditions? When will krypton-85 be produced?

YAMAMOTO: The krypton recovery plant of Tokai will be completed in 1982. At the middle of the year, krypton-85 will be recovered. The storage system using adsorbent is anticipated a few years later than the recovery plant.

PRELIMINARY SAFETY EVALUATION OF A COMMERCIAL-SCALE KRYPTON-85 ENCAPSULATION FACILITY*

A. B. Christensen, J. E. Tanner, and D. A. Knecht

EXXON NUCLEAR IDAHO COMPANY
P. O. Box 2800
Idaho Falls, Idaho 83401

Abstract

This paper demonstrates that a commercial-scale facility for encapsulating krypton-85 in zeolite-5A or glass at a 2000 MTHM per year nuclear fuel reprocessing plant can be designed to contain fragments and the 340 to 850 kCi krypton-85 inventory from an assumed catastrophic failure of the high pressure vessel. The vessel failure was assumed as a worst case and was not based on a detailed design evaluation or operating experience. The process design is based on existing commercial hot isostatic pressing technology operated at up to 40 times the scale required for krypton encapsulation. From the calculated process gas inventory in the pressure vessel and vessel design, the maximum explosive energy of 8.4 kg TNT and resulting vessel plug and fragment velocities were calculated. The facility Containment Cell housing the high pressure vessel was designed to contain the gases, fragments, and the shock wave energy calculated for a hypothetical vessel failure. The Access Cell located directly above the Containment Cell was designed to be a tertiary confinement of krypton-85, should the access hatch be breached.

I. Introduction

Krypton-85 is formed in moderate yield during nuclear fission of uranium or plutonium.[1] Most of it is trapped in the spent fuel and will not be released until the fuel is dissolved during reprocessing.[1] However, Federal regulations prohibit release of more than 50000 Ci of krypton-85 per gigawatt-year of electric power produced from nuclear fuel irradiated after January 1, 1983.[2] Thus krypton-85 must be recovered during fuel reprocessing,[3] and approximately less than 15% of the krypton-85 produced in light water reactors can be released during recovery and storage.[2]

One of the possible storage methods involves krypton encapsulation in zeolite 5A and low density glass at pressures near 2000 atm and respective temperatures of 600 and 950°C, producing volumes of

* Work performed under USDOE Contract DE-AC07-79ID01675.

immobilized krypton equal to volumes of krypton pressurized at about 30 atm.[4-6] Leakage rates were estimated to be less than 1% in ten years at storage tempertures of 300°C for zeolite 5A, and low density glass.[4-6] Hot isostatic pressing (HIP) technology, which has been developed recently to fabricate ceramic and metal alloy forms on a commercial production scale using active volumes of 30 to 2000 L and pressures and temperatures of 2000 atm and 1400°C, respectively, is directly applicable to the krypton-85 encapsulation process, using less than 50 L active volumes.[4,7,8,9]

High pressure systems contain a large amount of potential energy in the form of compressed fluids. Catastrophic failure of high pressure components, such as vessels, can result in damage to the surroundings as the potential energy is converted to kinetic energy of fragments.[10,11] Vessel design, maintenance, and routine inspection are used to help prevent catastrophic failure from occurring.[11-14] Barricades are generally used to contain energetic fragments and shock waves and to protect the rest of the facility.[11,15]

This paper will evaluate the consequences of a worst-case accidental rupture of a pressure vessel used to encapsulate krypton-85 at a commercial fuel reprocessing facility. It will demonstrate that it is feasible to ameliorate the effects of catastrophic vessel failure and to contain vessel fragments and krypton-85 in the facility.

A preliminary design of the encapsulation facility and the effects of a maximum credible accident will be described. The design requirements of the barricade and Containment Cell which will prevent release of krypton-85 will be given. Such requirements can be met within existing high pressure technology.

II. Description of a Commercial-Scale Krypton-85 Encapsulation Facility

Basis for a Commercial-Scale Facility

The reference commercial spent fuel reprocessing plant is assumed to be the one described in the draft environmental impact statement on waste management, with the exception that 100% krypton-85 recovery efficiency instead of 90% is assumed, to provide a conservative estimate.[16,17] The commercial-scale encapsulation facility will encapsulate 18.7 MCi per year of krypton-85 in zeolite 5A or glass, assuming that the facility operates at 110% of capacity for 300 days per year. The probable krypton-85 compositions obtained from cryogenic distillation and liquid fluorocarbon krypton-85 recovery systems can each be encapsulated.

Process Description

A simplified schematic of the encapsulation process is shown in Figure 1; more detail can be found in ENICO-1011.[4] The major equipment includes an internally heated pressure vessel similar to a HIP vessel, compressors, and vacuum pumps. The pressure vessel is

filled with a capsule containing the solid encapsulation substrate (zeolite 5A or glass), pressurized with krypton-85, and heated for a time sufficient to load the solid with krypton. After the encapsulation time is reached, the remaining krypton-85 is recycled to the storage containers using the compressors and vacuum pumps. The vessel is then opened, and the encapsulated sample removed in its container and placed in interim storage prior to removal to a permanent storage facility. A fresh batch of zeolite or glass is placed in the vessel and the process repeated. Based on laboratory studies, the process can be completed at a rate of one or more batches per day.[4-6]

Facility Design

The preliminary design for a krypton-85 encapsulation facility is shown in Figure 2; more detail can be found in ENICO-1055[7]. The building consists of three levels: a ground level, a first basement level, and a second basement (or subbasement) level. The pressure vessel and barricade are contained in an air-tight cell - the Containment Cell - in the second basement level; all of the other process equipment is located in the first basement level. The ground level is used for access to the process cells and for offices and support laboratories.

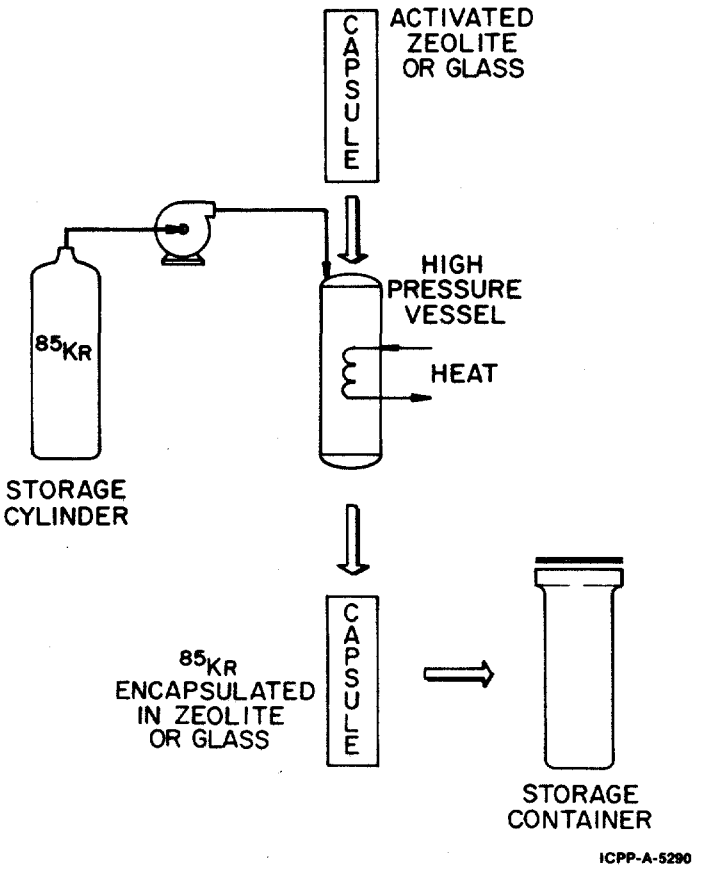

Figure 1. Simplified schematic of krypton-85 encapsulation process.

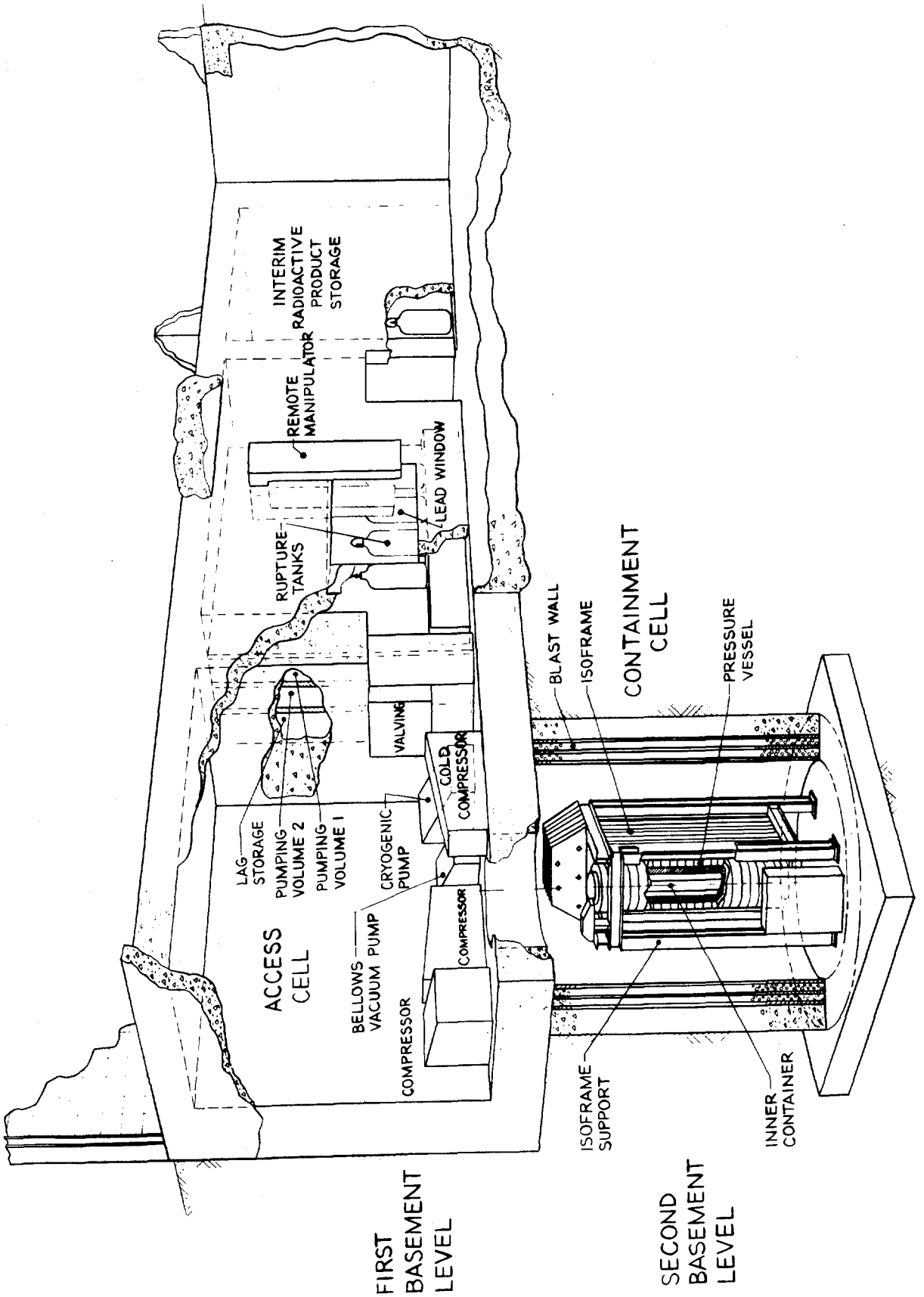

Figure 2. Preliminary isometric lay-out design of a commercial-scale krypton-85 encapsulation facility

III. Preliminary Safety Evaluation

This preliminary safety evaluation assumes that the worst possible consequence of operating a krypton-85 encapsulation facility would be the catastrophic release of krypton-85 to the surroundings. Based on the facility design shown in Figure 2, a number of potential sources of krypton-85 release exist in the facility. A detailed safety analysis of the probability of krypton-85 release from each of the sources has not been made. It is assumed that the high pressure vessel is the major source of a large, catastrophic release of krypton-85 because of the large inventory of krypton-85 in the vessel during an encapsulation run and because of the possibility that a vessel rupture could produce high energy fragments which could damage the facility and thus lead to release to the environment.

Postulated Maximum Credible Accident

Based on this preliminary assessment, the maximum credible accident for a commercial-scale krypton-85 encapsulation facility is assumed to be catastrophic rupture of the high pressure vessel during an encapsulation run. Modes of pressure vessel failure include: 1) failure of the plug or closure mechanism, 2) pressure vessel fracture in a radial plane (perpendicular to the longitudinal axis) producing two large fragments, and 3) pressure vessel fracturing into equal longitudinal strip fragments. The most severe effects will be used to design a containment barricade.

A detailed design study combined with a periodic inspection program of an operating vessel for a commercial-scale encapsulation system may show that the probability for vessel rupture is so low that it is not credible.[12-14] If other accidents are found to have a more significant risk than vessel rupture, some of the facility design criteria required to contain krypton-85 from vessel rupture should also be sufficient to contain krypton-85 from another source.

Critical Process Component

Based on the postulated maximum credible accident of catastrophic vessel rupture, the critical process component is the 318.6-L pressure vessel, shown in Figure 3. It is located in the Containment Cell of Figure 2, and uses a balanced pressure concept: the strength-bearing wall of the outer vessel is pressurized with an inert, non-radioactive gas, such as He or Ar, to balance the pressure of krypton-85 in the 50.5-L inner vessel.[18] Using standard HIP technology, the inner vessel containing the zeolite or glass and krypton-85 is heated to the encapsulation temperature of 500-1000°C, while the strength-bearing outer vessel is kept at less than 200°C. The tubing connection to the inner vessel would be closed remotely by crimping and welding after an encapsulation run, and the inner vessel could become the final storage canister.

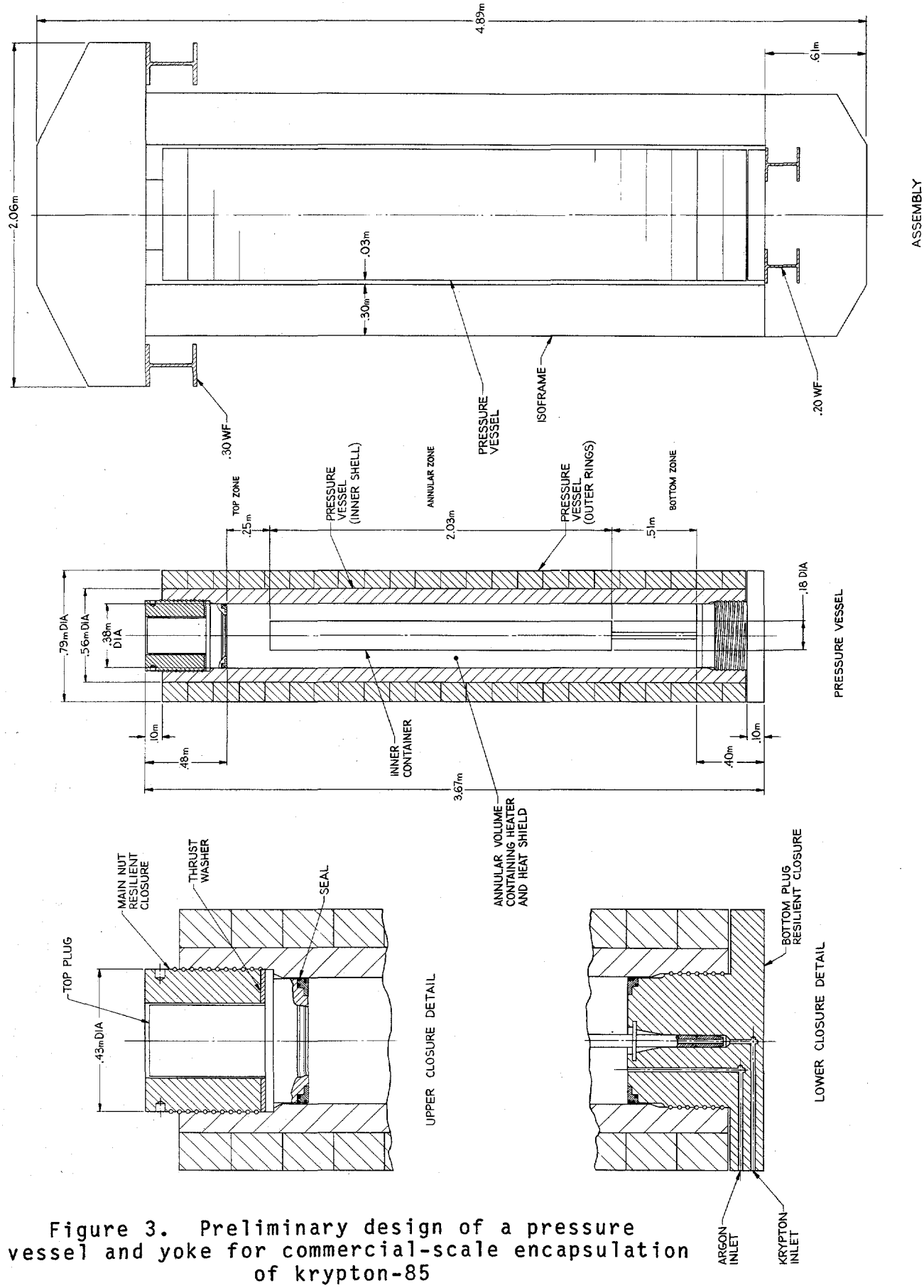

Figure 3. Preliminary design of a pressure vessel and yoke for commercial-scale encapsulation of krypton-85

Consequences of Postulated Maximum Credible Accidents

Using the design of the pressure vessel shown in Figure 3, it is possible to calculate the amount of gas contained in the vessel during an encapsulation run, the explosive pressure-volume energy of the compressed gas, and the resulting missile velocity, shock wave energy, and equivalent static pressure after a failure.

Amount of Compressed Gas in Vessel. The volume surrounding the inner canister contains argon gas and the furnace, consisting of a heater and a heat shield. Since the inner vessel is heated to the run temperature and the outer pressure vessel wall is kept below 200°C, the argon gas is at some intermediate temperature. Assumptions of the average temperature can be made for various regions of the vessel.[7] The inner canister contains zeolite 5A spheres or porous glass rods, 1 cm in diameter, with the respective void volumes of 25 L at 500°C and 13 L at 1000°C. The amounts of argon and krypton-85 in the pressure vessel during an encapsulation experiment at 500°C for zeolite 5A and 950°C for glass and 2000 atm can be calculated using the above assumptions and the Redlich-Kwong equation of state and are shown in Table I.[4,19,20]

Table I. Results of Calculations of Gas Compression Energy[a]

	Glass Encapsulation	Zeolite 5A Encapsulation
p_1,[a] atm	2000.	2000.
v_1, cm³/mole	55.1	47.5
T_1, K	782.	632.
p_2, atm	1.3	1.2
v_2, cm³/mole	1800.	1200.
T_2, K	40.	35.
Argon, m³ at STP	111.0	130.1
Krypton, m³ at STP	3.8[b]	9.5[c]
Total Gas Volume, m³ at STP	114.8	139.6
ΔU, MJ	37.8	29.3
ΔU, kg TNT	8.4	6.5

a Subscripts 1 and 2 refer to initial and final states, respectively.

b Assuming a 13-L void volume in the 50.5-L inner vessel; this is equivalent to 340 kCi of 6% ^{85}Kr in krypton.

c Assuming a 25-L void volume in the 50.5-L inner vessel; this is equivalent to 850 kCi of 6% ^{85}Kr in krypton.

Explosive Characteristics of Vessel Rupture. Using the vessel design shown in Figure 3 and the calculated volume of gas in the vessel at high pressure, the explosive energy, ΔU, of the vessel rupture can be calculated by assuming that the gas expands reversibly

and adiabatically to atmospheric pressure. The initial and final values of pressure, volume, and temperature as well as the calculated energies are shown in Table I.[11,21] The details of the calculations are shown in ENICO-1055.[7]

The maximum total energy which can be released from the compressed gas was calculated to be 8.4 kg TNT by assuming the conditions corresponding to glass encalsulation.[11] If Zeolite 5A encapsulation is assumed, the value is 6.5 kg TNT. Since the safety code developed by the High Pressure Technology Association states that above 100 atm considerable error in the energy results from assumption of the ideal gas behavior,[11] the Redlich-Kwong equation of state was assumed in the calculation. Using the methodology in reference 21, 5.7 to 22.2 kg TNT is obtained.[21] The Sandia Pressure Safety Manual uses the real gas properties of argon for calculating the 8.1 kg TNT energy, but assumes argon to be at room temperature.[22] Thus, the value used in this report is 37.8 MJ or 8.4 kg TNT, which is calculated for the vessel design in Figure 3, based on real gas properties of argon.

Facility Design Required to Ameliorate Effects of Maximum Credible Accident

The design of a commercial-scale krypton-85 encapsulation facility must include engineered safety features to contain fragments and krypton-85 released from the pressure vessel rupture assumed as the maximum credible accident. The vessel must be located within a sealed Containment Cell with provisions for recovery of released krypton-85. The Containment Cell must itself be protected from fragment or blast damage. Secondary restraint on the vessel closure by a passive yoke structure around the vessel would further limit fragment damage and would make launching of the plug an incredible event.

The calculations of fragment energy and shock energy for several modes of fragmentation are shown in Table II. The facility design features required to ameliorate the explosive effects described in the following section are based on the values shown in Table II. Detailed calculations are given in ENICO 1055.[7]

When a small number of fragments is formed, most of the energy is removed by the kinetic energy of the fragment. When a large number of fragments is formed, most of the energy is removed by the shock wave energy. Thus the Containment Cell must be designed with wall and missile shield thicknesses which are large enough to contain both a launched plug fragment and the maximum shock energy obtained from a multiple fragmentation mode.

Pressure Vessel. The pressure vessel (Figure 3) is a multi-walled shrunk-fit 318.6-L vessel with threaded end closures containing a 50.5-L active volume. This type of vessel is commonly used in commercial high pressure and temperature applications, such as Hot Isostatic Pressing.[8,9] The vessel contains a heater/heat shield package in the annulus between the inner wall of the pressure vessel and the inner vessel containing the zeolite or glass.

Table II. Explosive Energy of Vessel Fragmentation[a]

	Fragmentation Mode			
	Plug	2 Parts	10 Parts	100 Parts
Fragment Quantity:				
Mass, kg	548	5933	1186	119
Area, m^2	0.15	0.49	0.49	0.49
Kinetic Energy, MJ	22.7	11.3	0.76	0.08
Velocity, m/s	288	61.8	35.7	35.7
Concrete Thickness, m	1.6	0.55	0.04	0.004
Steel Thickness, m	0.13	0.05	0.003	0.0003
Shock Wave Energy, MJ	15.1	15.1	30.2	30.2
Equivalent Static Pressure in Containment Cell,[b] atm	3.6	3.6	5.9	5.9
Equivalent Static Pressure in Containment Plus Access Cells,[b] atm	0.7	0.7	1.1	1.1

a See ENICO-1055 for details of the calculations.[7]

b Equivalent static pressure is the pressure measured relative to atmospheric pressure which, when maintained indefinitely in the contained volume, will produce the same deflections in the walls as the shock wave.[11]

Penetrations for gas lines and instrument and electrical leads are located on the bottom closure plug. The internal volume and pressure-bearing wall of the pressure vessel are instrumented with pressure and temperature sensors to provide indication and/or alarm for operating conditions.

Safety Yoke and Support. The safety yoke shown in Figure 3 is a massive band structure that surrounds the pressure vessel during high pressure operation. The yoke provides secondary closure force in the event of failure of the threaded closure, and its sides also provide missile barriers on two sides of the vessel.

The vessel and yoke are mounted on a support structure which has rails for moving the yoke out of position for loading and unloading the vessel. Microswitches and interlocks are provided to prevent pressurization of the vessel when the yoke is not in the operating position. A hydraulic system is used for remote positioning of the yoke.

Calculations of the static and dynamic load on the yoke which would result from plug failure give safety factors, based on the ultimate strength, of 7.4 for the static load and 1.4 for the dynamic load assuming ASTM A-242 as the yoke material.

Containment Cell. The Containment Cell shown in Figure 2 is a cylindrical cell, 3.7 m diameter by 5.5 m high, constructed of 1.6-m thick reinforced concrete with an airtight steel liner and is located in the second basement level. Access to the pressure vessel for loading and unloading the zeolite or glass container is through a sealed overhead cell access cover located in the Access Cell in the first basement level. The Containment Cell will contain any krypton-85 released. Piping to and from the cell is used for purging the cell and recovering krypton-85.

The values of fragment mass and velocities and shock wave energy resulting from pressure vessel rupture shown in Table II were used to design the concrete thickness of the walls, floor, and ceiling shown in Figure 2. The access cover requires twelve 3.8-cm diameter bolts to contain the shock wave and equivalent static pressure.

Explosive Barrier and Missile Shield. The explosive barrier is a cylindrical composite structure which lines the cell wall, shown in Figure 2 and surrounds the pressure vessel.[23] It is constructed of screen materials sandwiched between perforated steel plates and is designed to suppress a 20-kg TNT blast. Structural angles mounted on the inside and outside walls serve as missile and shock wave deflectors. The missile barricade also serves as a shock wave suppressor. This type of barricade is a safety-approved suppression shield for fragment containment, blast suppression, and flame attenuation.[23]

The 13-cm steel missile shield located above the high pressure vessel (Figure 2) is suspended from the ceiling of the containment cell and protects the cell liner from missiles resulting from vessel rupture. The 1.6-m thick concrete ceiling wall is also thick enough to stop the vessel plug, if necessary.

Quality Assurance. The development of a Quality Assurance Program Plan is essential for control of design, material fabrication, testing, and operation of the krypton-85 encapsulation facility. The plan should define responsibilities for establishing requirements and assuring compliance with the requirements.

Design, fabrication, and inspection of the pressure vessel should be in accordance with the rules of the ASME Boiler and Pressure Vessel Code Section III or Section XIII Division 2. Other applicable codes should also be consulted.[11]

An explosive model test program should be carried out to determine or verify vessel failure modes, fragmentation, missile velocities, and adequacy of barriers and containment designs.

IV. Conclusions

This paper demonstrates that a commercial-scale krypton-85 encapsulation facility can be designed to contain fragments and the 340-850 kCi krypton-85 inventory from a hypothetical catastrophic failure of the high pressure vessel.

The pressure vessel, containing an active volume of 50 L, is designed to encapsulate the 17 MCi annual krypton-85 production from a 2000 MTHM commercial spent fuel reprocessing plant in 300 days/yr, assuming 110% production overcapacity. The vessel design is based on existing commercial hot isostatic pressing vessel technology in which the active volumes range from 30 to 2000 L.[8] Although vessel rupture is an unlikely event if modern design and inspection procedures are used,[11-14] it is assumed to be the maximum credible accident for the evaluation in this report.

The facility, which is designed to contain vessel fragments and krypton-85 from a hypothetical vessel rupture, consists of one aboveground and two underground levels of cells. The process vessel is located in a sealed second basement level Containment Cell, which is designed to be a secondary containment for the process gases, argon, krypton, and krypton-85. The first basement level houses process equipment such as manipulators, cranes, compressors, vacuum pumps. Feed gas storage, and interim product storage for encapsulated krypton-85 are also on this level. The Access Cell, which contains the access to the second basement level Containment Cell, is also sealed and is designed to provide tertiary containment of the krypton-85 if the connecting wall to the Containment Cell is breached. The aboveground level houses offices, a support laboratory, and access hatches to the basement cells.

The inventories of argon and krypton-85 in the high pressure vessel during an encapsulation run would produce a maximum explosive energy in the Containment Cell of 37.8 MJ or 8.4 kg TNT. The explosive barrier is designed to suppress a 20 kg TNT blast.[23] The 1.6-m thick ceiling and the bolted hatch cover of the subbasement Containment Cell are designed to contain the 30 MJ or 6.7 kg TNT shock wave.[11] A 13-cm thick steel missile barrier and support structure above the pressure vessel is the required size to contain a launched 548-kg vessel plug at a velocity of 288 m/s estimated for plug failure.[11] However, a yoke surrounding the vessel would make plug launching an incredible event. Other smaller fragments would be contained by the surrounding explosion barrier and the second basement level cell walls supported by the surrounding ground.

After a more detailed design of the krypton-85 encapsulation facility is made, further safety evaluations should be carried out to identify all accidents and determine probability and consequences of each. Such an evaluation may show that vessel rupture is not a credible accident and that facility design requirements to contain krypton-85 from the maximum credible accident will not be as stringent. However, the preliminary evaluation shown in this report should give a first approximation to the design requirements for a commercial-scale krypton-85 encapsulation facility.

Acknowledgment

The assistance of R. C. Green, L. H. Jones, and J. P. Sekot in the preparation of this report is gratefully acknowledged.

References

1. National Council on Radiation Protection and Measurements, Krypton-85 in the Atmosphere -- Accumulation, Biological Significance and Control Technology, NCRP Report No. 44, Washington, D.C. (July 1, 1975).

2. "Environmental Radiation Protection Standards for Nuclear Power Operation," Federal Register, 42, No. 9, Part VII, 2858 (January 13, 1977).

3. Alternatives for Managing Wastes from Reactors and Post-Fission Operations in the LWR Fuel Cycle, ERDA-76-43, Vol. 2, Chapt. 14.1, 14.1-14.7 (April 1976).

4. R. W. Benedict et al., Technical and Economic Feasibility of Zeolite Encapsulation for Krypton-85 Storage, ENICO-1011 (September 1979).

5. R. D. Penzhorn et al., "Long-Term Storage of Krypton-85 in Zeolites," Proc. Int. Symp. Management of Gaseous Wastes from Nuclear Facilities, IAEA-SM-245, Vienna (February 1980).

6. G. L. Tingey et al., "Solid State Containment of Noble Gases in Sputter Deposited Metals and Low Density Glasses," Proc. Int. Symp. Management of Gaseous Wastes from Nuclear Facilities, IAEA-SM-245/31, Vienna (February 1980).

7. A. B. Christensen, J. E. Tanner, and D. A. Knecht, Preliminary Safety Evaluation of a Commercial-Scale Krypton-85 Encapsulation Facility, ENICO-1055 (September 1980).

8. F. X. Zimmerman, "HIP Equipment for Industrial Applications," Metal Powder Report, 35, 300 (July 1980).

9. H. D. Hanes et al., Hot Isostatic Processing, MCIC-77-34 (November 1977).

10. J. F. Pittman, Blast and Fragments for Superpressure Vessel Rupture, NSWC/WOL/TR 75-87 (February 1976).

11. High Pressure Technology Association, High Pressure Safety Code (Brentford, Middlesex, England: F. J. Milner and Sons, 1977).

12. V. C. D. Dawson, "Safety and Safety Codes," I. L. Spain and J. Paauwe, eds., High Pressure Technology, Vol. I (New York: M. Dekker, Inc., 1977), pp. 29-49.

13. D. E. Witkin and G. J. Mraz, "Design Philosophy of Pressure Vessels for Service Above 10 ksi (70 MPa)," Trans. ASME, Pressure Vessel Technol., 76-PVP-62, 1 (1976).

14. T. A. Smith and W. A. Warwick, "Survey of Defects in Pressure Vessels Built to High Standards of Construction," J. T. Fong, ed., Inservice Data Reporting and Analysis for Pressure Vessels, Piping, Pumps, and Valves, PVP-PB-032 (New York: ASME, 1978), pp. 21-53.

15. W. E. Lawrence and E. E. Johnson, "Design for Limiting Explosion Damage," Chem. Eng., 96 (January 1974).

16. Management of Commercially Generated Radioactive Waste, Draft Environmental Impact Statement, DOE/EIS-0046-D (April 1979).

17. Technology for Commercial Radioactive Waste Management, DOE/ET0028, Vols. 2 and 3 (May 1979).

18. J. M. Bertz, "Method of Storing Gases," U. S. Patent 4158639, (June 1979).

19. K. K. Shaw and G. Thodos, "A Comparison of Equations of State," Ind. Eng. Chem., 57, 30-37 (1965).

20. R. Simonet and E. Behar, "A Modified Redlich-Kwong Equation of State for Accurately Representing Pure Components Data," Chem. Eng. Sci., 31, 37-43 (1976).

21. W. E. Baker et al., Workbook for Predicting Pressure Wave and Fragment Effects of Exploding Propellant Tanks and Gas Storage Vessels, NASA-134906 (September, 1977).

22. Pressure Safety Practices Manual of Sandia Laboratories, SLA-73-0065 (January 1973).

23. R. C. Green, EG&G Idaho Company, Inc., Idaho Falls, ID, Private Communication (June 1980).

EXPERIMENTAL DEVELOPMENT AND DESIGN ASPECTS OF A ^{85}KRYPTON REMOVAL DISTILLATION UNIT

G.E.R. Collard, L.P.M. Geens, P.J. Vaesen, W.R.A. Goossens
S.C.K./C.E.N., Mol, Belgium

Abstract

Cryogenic distillation as a method for the removal of krypton from gaseous effluents of reprocessing plants has been studied with non active gases at the pilot scale of up to 0.010 $kg.s^{-1}$ through-put (30 STP $m^3.h^{-1}$), in a packed bed configuration. Pressure and temperature of the feed, reflux rate, heating power of the kettle of the column are the most important parameters which have been studied in order to avoid crystallisation of xenon in the precoolers as well as formation of solid phase xenon-nitrogen mixtures in the column. The use of a simple thermal regulation system, based on the narrow separation front of two components, made it possible to fulfil the mass- and heat-balances in order to condense variable quantities of noble gases, representing a mean accumulation to feed mass ratio of down to 0.01 %. The unit has continuously worked troubleless during more than 13,000 hours with an average availability factor of 99.70 %. During this long campaign supply of cooling nitrogen appeared to be the most critical part of the unit. Indeed, during 0.20 % of the time the unit had to be worked batchwise for its maintenance.

It appears that nitrogen containing up to 1 % argon, 10 to 2000 ppm krypton and up to 8000 ppm xenon can be continuously treated by distillation acquiring large krypton decontamination factors without any problems due to the high xenon concentration and without accumulation of other compounds than xenon and krypton in the kettle of the column.

I. Introduction

Since 1976 the Belgian Nuclear Research Center, S.C.K./C.E.N., in association with S.A. BELGONUCLEAIRE, BN, has investigated the removal of krypton from simulated fuel dissolver off-gases by means of distillation at low temperature.

The process retained consists of a continuous removal of krypton and xenon from the carrier gas consisting of nitrogen and argon (1-2%) in a first distillation-rectification column, the bottom product of which is further splitted into krypton and xenon in a second distillation column working batchwise. No fundamental research was previously performed. This means that the whole installation has gradually been modified and improved according to the operational experience in order to get a well equipped unit, the upscaling of which to an actual reprocessing off-gas installation became feasible. This historical improvement of the experimental unit and the results finally obtained are described in this paper.

II. Historical evolution of the unit

After a commissioning campaign various modifications were brought to the first column, its peripherical lines and instrumentation in order to increase the nominal working pressure from 0.3 MPa to 0.8 MPa. Indeed it immediately appeared that a solid phase containing xenon was formed in the vicinity of the feed point of the column. Moreover a non-negligible part of the feed was liquefied in the precoolers causing important disturbances at the entry of the column so that it was impossible to keep the unit in thermal equilibrium.

After these modifications a continuous campaign of one month was performed in February 1977 in order to verify the decontamination performance of the first column and to get additional information for more developped automation of the process control system. Final modifications were performed and the unit was at last started up in November 1978 for an uninterrupted campaign until May 1980. During the 13,000 hours of operation the outage time due to uncontrolled phenomena amounted 35 hours, meaning an operation availability degree of 99.7 %. Most of the results presented here have been obtained during this period and during the summer of 1980.

III. Description of the flow diagram

A simplified flow diagram of the cryogenic unit is given in Fig. 1. Gas to be treated is fed at a constant pressure of 0.9 MPa into one of the two parallel three-compartment heat exchangers working alternatively. Herein the inlet gases flow countercurrently to the cold outlet gases and to the vapors of the liquid nitrogen used as coolant in the condensor of the first column. The cooling gases are previously slightly preheated in order to keep the feed at constant temperature at the entry of the column and to avoid desublimation of xenon and condensation of nitrogen in the coolers.

In the first packed distillation-rectification column operated at 0.8 MPa, xenon and krypton are continuously washed out with liquid nitrogen, refluxed at the column condensor. Cooling is performed by liquid nitrogen which is evaporated in a coil at 0.2 MPa. Heat- and mass-balances are kept in equilibrium by regulating the cooling in such a way that the krypton layers always reach the same height in the lowest part of the column packing. This leads to an almost constant temperature profile inside the column as shown in Fig. 2. Xenon and krypton accumulate in the kettle while argon and nitrogen leave the top of the column. When the quantity of liquid present in the kettle is large enough, a part of it is transferred in the second column wherein krypton and xenon are separated by batch distillation. This column is cooled by a closed loop of liquid nitrogen at 2 MPa which is refrigerated in a primary exchanger by liquid nitrogen at 0.2 MPa. This way of cooling avoids a too large desublimation of krypton, and thus an excessive accumulation of solid around the condensor of this column. Krypton is extracted under a high reflux rate at the top of the column until its concentration in the kettle is lower than 1 ppb. The bottom product xenon is then also transferred in a storage bottle. Both transfers are made in two steps. The first step consists of cryogenic pumping in bottles cooled by liquid

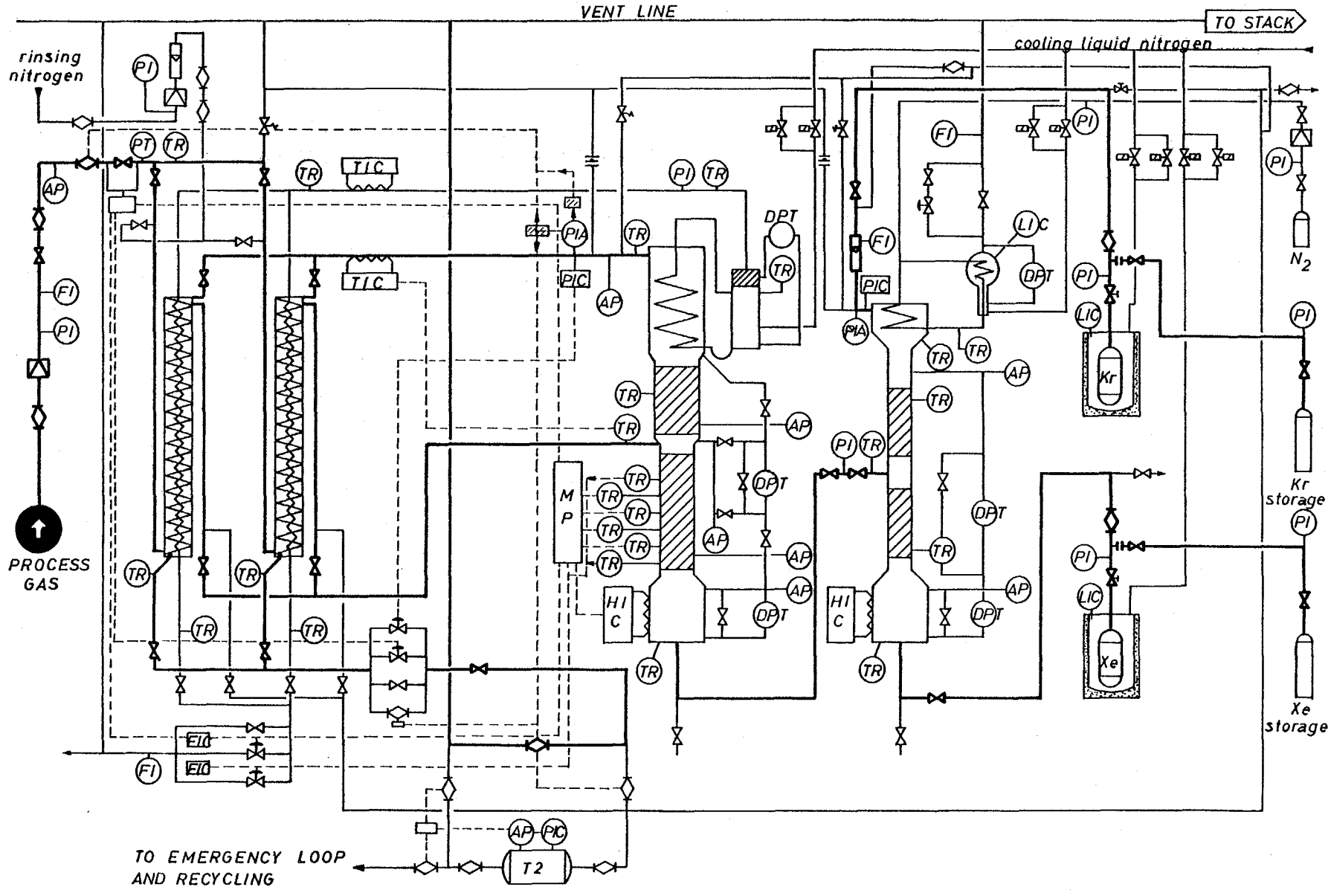

FIG.1: KRYPTON REMOVAL BY CRYOGENIC DISTILLATION

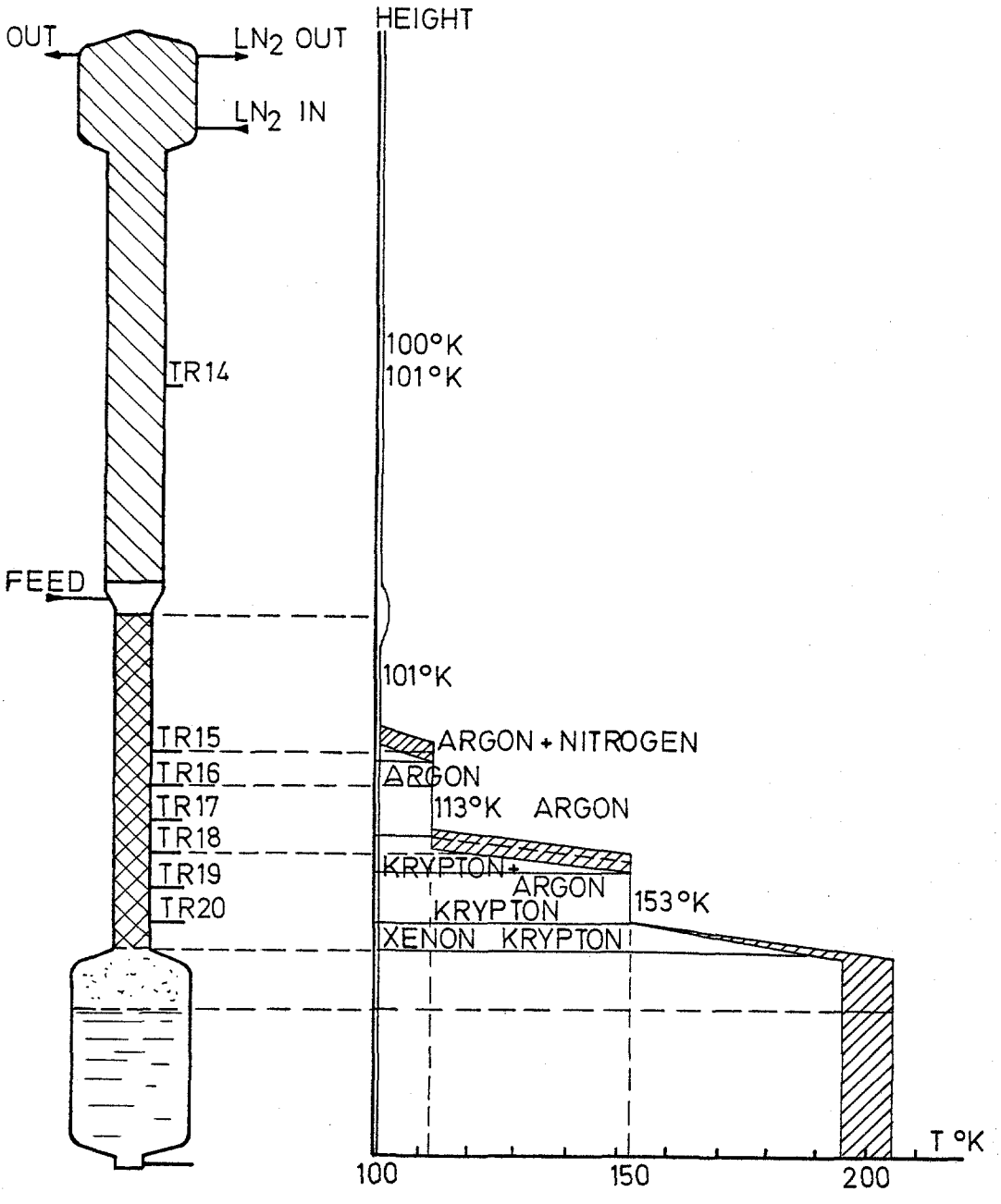

FIG.2: TEMPERATURE PROFILE IN THE FIRST COLUMN

nitrogen. After pumping the cooling of these bottles is stopped and their temperature increase causes an increase of the gas pressure. The gases are finally transferred in storage bottles under pressures up to 10 MPa. In the future krypton will be stored under lower pressure in bottles filled with sorbents.

In the case of insufficient krypton decontamination or of failure of the liquid nitrogen supply, the flow of process gases leaving the unit can be diverted to a emergency loop where it is stored under 2 to 3 MPa before being recycled for a second treatment.

The unit is also provided with safety valves, alarms and rupture disks, which make it safe.

IV. Description of some parts

Cold box

The two heat exchangers and the two columns are placed in a cold box filled with powdered perlite. Freezing of humidity and condensation of air in contact with the cooling loops is avoided by rinsing the whole box with nitrogen in slight underpressure.

Heat exchangers

The heat exchangers consist of three concentric copper tubes. Vapors of cooling nitrogen flow through the central one, process gas flows in the finned second pipe, while treated gas flows in the external tube.

Distillation columns

The columns consist of a kettle electrically heated, two beds of spring type rashig Rings 3x3x0.4 mm and a condensor of the coil type. The packing height in the first column (Fig. 3) amounts to 0.72 m in the upper part with an internal diameter of 0.10 m and to 0.80 m in the lower part with an internal diameter of 0.07 m. The lower part of the packing is equipped with thermoresistances which allow the determination of the local temperatures. A few of these thermoresistances are connected to a temperature control system in such a way that a constant temperature profile and consequently also the mass-balance equilibrium are maintained in the column. Continuous measurements of pressure drops in the column indicate potential pluggings due to solid phases in the packings.

The packing of the second column consists of two identical beds of 0.80 m height and 0.05 m diameter.

Process control and data acquisition

The performance of the first column is controlled by means of a hibrid system combining conventional analog and digital control systems.

The main flow of the cooling nitrogen is divided into two streams in the vapor phase. The primary stream flow rate is automatically adapted fully to changes in the feed rate and partly to changes of the heating power of the kettle. The secondary stream flow rate is adjusted to maintain the upper krypton layers in the vicinity of the TR 18 (or TR 16) temperature probe in the lower packing (Fig. 3). In nominal conditions the pressure is maintained constant by means of a PID-regulator at the outlet of the column. When the column is working in stand-by, the pressure is regulated by means of the cooling while the temperature indications provided by TR 18 are no longer taken in account.

The temperature of the feed is maintained constant by suitable heating of the cooling gases before they enter the heat exchangers. The temperature of the cooling nitrogen flow is kept a few degrees

above this of the treated process flow on which the regulation is applied. Control and regulation of the second column are rather simple. The pressure is kept constant by means of the cooling flow. No other control is needed for this column.

V. Experimental results and interpretation

Working limits of the unit

In order to increase the concentration of xenon in the feed without excessive problems due to the low solubility of xenon in liquid nitrogen, the pressure of the system has to be higher than 2 MPa (1). Such a pressure should not easily be accepted for radio-active gases, although the total gas content of the system is more than 1000 orders of magnitude lower than the liquid hold-up of the columns. Moreover the boiling point of nitrogen at 2 MPa is 116 °K, ten degrees below the critical temperature. The vicinity of these two temperatures could be an important source of hazards in case of failure of the cooling system.

Based on these considerations a lower working pressure has been retained and the operational limits of the system have been studied at 0.8 MPa.

Working conditions of the heat exchangers

When the partial pressure of xenon in the gas flow is higher than its vapor pressure at the outlet temperature, a solid phase containing xenon is formed on the cold walls of the heat exchanger. Comparison of xenon concentrations at the outlet of the heat exchanger with concentrations calculated by means of its vapor pressure above its solid phase (Table I) shows that pure xenon probably crystallizes. The equation of Freeman and Halsoy (2) has been used to calculate the vapor pressure of xenon :

$$\log_{10} P_s = 4.8563 - \frac{799.1}{T} \qquad (1)$$

where P_s is the vapor pressure of xenon (bars)
T_s is the temperature (K).

It is clear that the temperature at the outlet of the heat exchangers must be higher than the saturation temperature of xenon under the nominal ranges of total pressure and xenon concentration. Moreover the wall temperature may not be much lower than the saturation temperature and the cross-section of the tubes must be large enough to allow temporary crystallisation when during short times peaks of xenon concentration are present at the inlet.

Performance of the distillation-rectification column

At a total pressure of 0.8 MPa the boiling point of nitrogen is 100.38 K. The vapor pressure of xenon at this temperature is equal to 78 Pa corresponding to a concentration of 97.5 vol ppm, which is much lower than the nominal 1000 vol ppm concentration expected in reprocessing plant off-gases. Moreover the application of the model of Peng and Robinson (3) on the experimental results of Mastera (4)

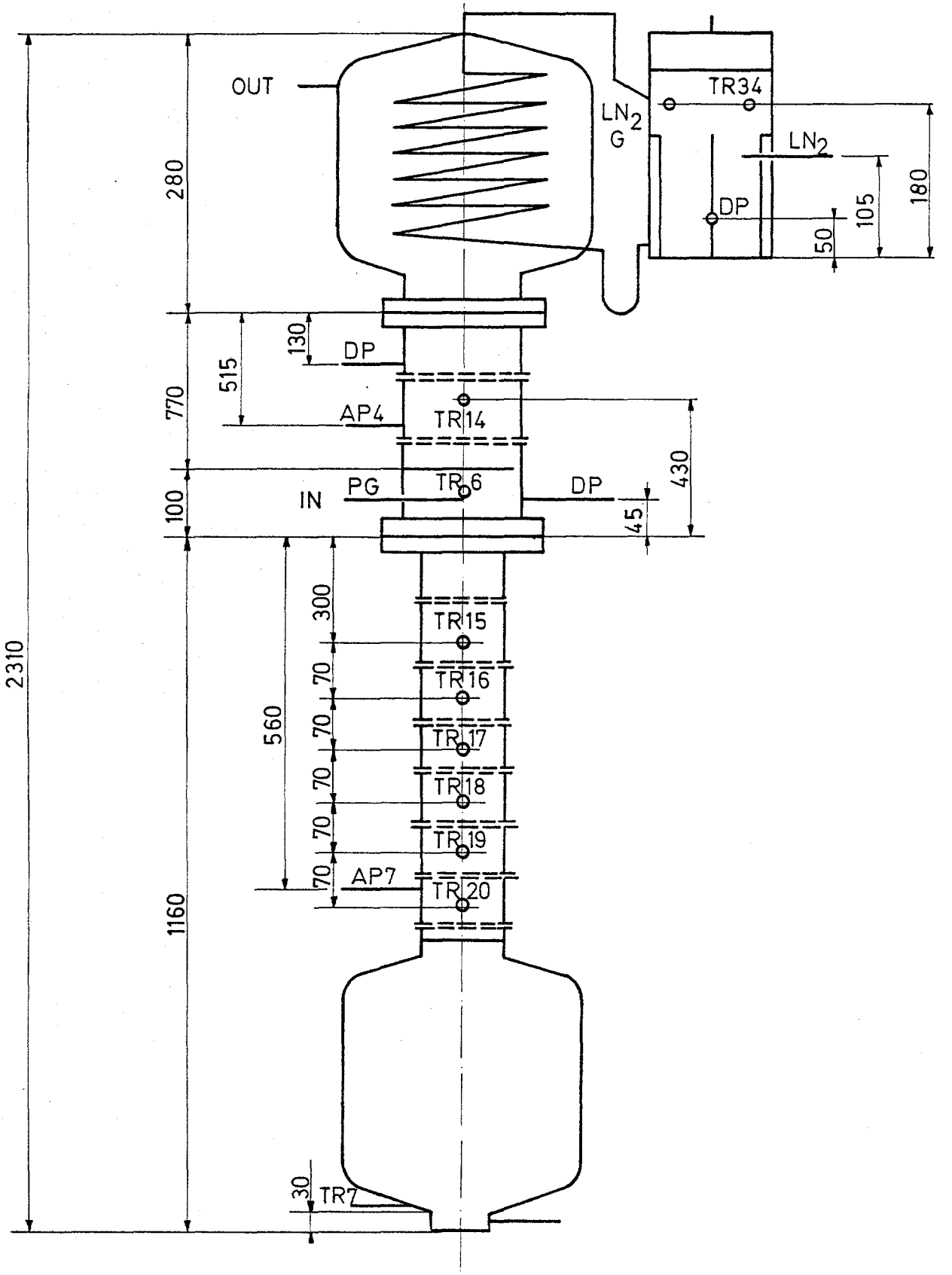

FIG.3:MAIN DIMENSIONS OF THE FIRST COLUMN

Table I. Maximum concentration of xenon at the outlet of the heat exchangers

Gas flow rate ($kg.s^{-1}$)	Temperature (K)	Concentration of xenon (ppm volume) experimental	F & H
$2.1 . 10^{-3}$	112	653	658
$2.1 . 10^{-3}$	113	763	761
$2.1 . 10^{-3}$	116	1076	1160
5.2 to $6.2 . 10^{-3}$	120	2066	1968
$2.1 . 10^{-3}$	121	1980	2234
5.2 to $6.2 . 10^{-3}$	125	3780	3634
$2.1 . 10^{-3}$	126	3897	4084

shows that binary mixtures of xenon and nitrogen have a triple point at 100.59 K with a liquid concentration of 1.14 mole % xenon corresponding to a concentration of 48.56 vol ppm in the gas phase (5). These values are lower than these calculated by R. von Ammon et al (1), namely a liquid concentration between 4 vol % (at 0.5 MPa) and 10 vol % (at 1 MPa) by means of the ideal solution model. Anyhow, according to both estimates, concentrations higher than 1000 vol ppm in the gas phase lead to a solid phase when an instantaneous equilibrium between the phases in the column is assumed. This prediction remains valid even if a large reflux rate is used in order to get some dilution in the gaseous phase. Consequently it is advisible to keep the reflux rate at a minimum value in such a way that the concentrations of xenon in the liquid phase remains lower than the triple point concentration.

As can be seen in Table II, dynamical working conditions too have an important effect on the behaviour of the column. In this table, the concentration of xenon in the refluxing liquor at the feed point has been calulated under the following assumptions : the xenon concentration in the gas phase ascending from the lower column part is negligible and the liquid flow rate in this lower column part depends only on the heating power of the kettle of the column.

These results show that the solubility of xenon in the liquid phase falling down in the column might probably be higher than 1.14 %, the value estimated by means of Peng and Robinson's model. At low feed rate the permissible liquid xenon concentration is obviously lower than at higher rates. This indicates that mass transfer is slower than heat transfer in these conditions and that xenon desublimation occurs directly in the gas phase. The solid xenon thus created accumulates in the column, due to its very poor dissolution rate. The design of the column must thus favorize the mass transfer in the vicinity of the feed point. This can be done by shortening the empty space length of the column located between the feed point and the first upper plate or the support plate of the upper packing.

Table II. Working limits of the column

Gas feed rate ($g.s^{-1}$)	Inlet gaseous Xe concentr. (vol. ppm)	Kettle heating power (W)	Reflux flow rate ($g.s^{-1}$)	Calculated liq. Xe concentr. (mole %)	Working time (h)
2.08	2634	100	0.63	0.87	15.25[1]
	5506	200	1.26	0.92	16.60[1]
	7206	250	1.58	0.95	10.50[1]
4.17	1869	100	0.63	1.22	$\geqslant$ 23
	2643	150	0.95	1.14	$\geqslant$ 17
6.25	1296	100	0.63	1.27	$\geqslant$ 23
	1826	150	0.95	1.19	$\geqslant$ 23.5
	2665	175	1.10	1.49	$\geqslant$ 19
8.33	1264	100	0.63	1.64	$\geqslant$ 24
	1164	150	0.93	1.03	$\geqslant$ 23

[1] Plugging caused by crystallization took place in the column after this time.

The efficiency of the krypton removal

Assuming ideal solutions and perfect gases, and also a relative volatility of nitrogen in the N_2-Kr system between 90 K and 110 K almost equal to $\alpha_{N_2,Kr} \approx 50$, it can be calculated that krypton decontamination factors of 100 and 1000 can be achieved by respectively 4 and 5 transfer units for a reflux ratio of 0.25 at a gas feed rate of 8.3 g/s (24 STP $m^3\ h^{-1}$) at a temperature of 130 K.

Since, the Rashig rings used as packing material have a length of a transfer unit of about 3 cm in these working conditions, decontamination factors of 100 and 1000 can been achieved with packing lengts of respectively 12 and 15 cm. Nevertheless, one has to keep in mind that the lowest layers of the packing are used for heat transfer and that the liquid flow rate in them varies from a very low value corresponding to the reflux in the enrichment part of the column (0.93 g s^{-1} for a heating power of 150 W corresponding to a reflux ratio of 0.12 in the upper part) to the desired value. Experimental values of krypton concentration in the feed (AP_0), in the column at the feed level (AP_2) and for packing heights of 20 cm (AP_4) and 72 cm (AP_1) are summarized in table III.

These values indicate that DF's higher than 500 are already obtained with a packing height of 20 cm. Nevertheless, earlier experiments have shown that this performance can only been achieved if the regulation of the cooling system maintains a rather constant liquid flow rate in the column. Indeed, decreasing cooling implies both decreasing reflux and increasing gas flow in the column. In practice, the variations in the cooling power must be lower than 10 % of the reflux, and the lowest value of the cooling power must remain between 90 and 99 % of the kettle heating power.

Table III. Krypton concentration at different points

Feed ($g s^{-1}$)	Heating power (W)	Feed temperature (K)	Cooling nitrogen ($g\ s^{-1}$)	Krypton concentration (vol. ppm) AP_0	AP_2	AP_4	AP_1
2.1	100	121	1.5	148	149	< 0.2	< 0.2
2.1	200	124	2.1	225	223	< 0.2	< 0.2
2.9	100	120	2.1	63.5	n.m.	n.m.	< 0.2
2.9	100	120	1.8	900	n.m.	n.m.	< 0.2
4.13	100	120	2.0	760	n.m.	n.m.	< 0.2
6.25	102	120	2.1	1000	n.m.	n.m.	< 0.2
6.25	102	120	2.1	2100	n.m.	n.m.	< 0.2
6.25	102	116	1.6	90	140	< 0.2	n.m.
6.25	101	126	2.3	90	139	< 0.2	n.m.
6.25	200	116	2.4	97	96	< 0.2	< 0.2
10.5	100	120	2.7	873	n.m.	n.m.	< 0.2

Conclusion

The critical points of the design of a cryogenic distillation unit for krypton removal from dissolver off-gases have been examined in such a way that this method can be applied for this application and for others such as removal of xenon from reactor off-gases, even when xenon concentrations are as high as a few tenths of percent in the feed.

Such a unit will be built in the off-gas loop of the Head-End Research Mock-up on an Engineering Scale, called HERMES under construction at S.C.K./C.E.N.

Active krypton storage will also be studied with this new unit.

Aknowledgment

The authors thank all the people who worked on this study and expecially M. De Smet, E. Ooms, J. Stevens and D. Hennart, G. Pauluis, A. Zahlen who operated the unit.

References

(1) von Ammon R. et al ; Die Entwicklung der Abtrennung von Kr-85 aus dem Abgas von Wiederaufarbeitungsanlagen, KfK-Nachrichten, 11, 3, 19-24 (1979).

(2) Freeman M.P. and Halsey G.D. ; The solid solution krypton-xenon from 90 to 120 K, the vapor pressures of argon, krypton and xenon; J. Phys. Chem., 60, 1119 (1956).

(3) Peng D.Y. and Robinson D.B. ; A new two-constant equation of state, Ind. Eng. Chem., Fundam., 15, 59 (1976).

(4) Mastera S.-G.J., Dampf-Flüssig-Gleichgewichtsdaten der Systeme Ar-N_2, Kr-Ar, Kr-N_2 und Xe-Kr sowie Löslichkeitsgrenzen des festen Xenons und des festen Kryptons in flüssigen Luftkomponenten, Jül-1380 (1977).

(5) Gosset R. ; University of Liège ; Personal communication (1980).

DISCUSSION

v. AMMON: I just want to mention that we very recently have obtained experimental data on the solubility of xenon in liquid nitrogen. These experiments were carried out at the Technical University of Berlin. Indeed, the solubility is much lower than that which is calculated ideally. Just to give a number, at 95K it amounts to approximately 1%, whereas if you calculate it ideally, it is of the order of 25%. So, this explains some of the results which you obtained, and we at Karlsruhe have obtained them, also.

PENCE: You indicated what you thought would be the limits with regard to xenon and krypton. You have processed it, so I am sure you looked at it and have done the calculations. Can you share with us what you think is the rate of change you can tolerate? Do you think you can tolerate the anticipated range of changes from the dissolver cycle? Do you have any problems in that regard?

COLLARD: In fact, it is very easy to change the flow rates, and we do change them. Therefore, we use a potentiometer and a mass flow meter for the flow rate. If you change the potential, it takes about 10 seconds to reach 90% of the variation and the whole automated system can follow it, including the cooling. It is just the same for the concentration. Perhaps for the larger peaks of xenon combined with a decrease of the gas flow rate, it will take a longer time. Therefore, we in our facility, have installed a tank of about 1 m^3 just upstream of the distillation column to avoid these peaks. Normally, you may change from 1,000 to 8,000 ppm, without any problems. If the regulation of temperature in the heat exchanger can't follow the change, it can be a problem. If you use electrical heaters, the resistance is rather low and so the response of your electrical heating can be rather slow, too. But it is the only problem. It is a question of choice of your heating element.

PENCE: Then, you think the column temperature adjustment is more critical than the reflux flow rate?

COLLARD: The temperature at the inlet perhaps. But it is regulated by the temperature in the heat exchanger. Thus, if you have an increase in pressure you have, first, a desublimation in the heat exchanger, which can be used as a buffer to maintain the operation of the column. So, it is a very good thing. But if this peak remains during a long period, you can have a plugging of your heat exchanger. So the column response is very good, because 1,000-8,000 ppm does not change the thermal balance but very little. But you have to be sure the temperature in your heat exchanger can follow the variation of concentration.